The Analysis of The Glaciolacustrine Sediments of Lake Caserococha, Peru

by

Jeri D. Wackler

A senior thesis submitted to fulfill
the requirements for the degree of
B.S. in Geology, 1985

The Ohio State University

Thesis Advisor

Lawrence Krissek
Department of Geology
and Mineralogy

ABSTRACT

Glaciolacustrine sediments are ideally-suited for paleoclimatic studies because these sediments are deposited continuously in freshwater lakes of glacial origin, and usually remain undisturbed for many thousands of years. Previous studies of clastic sediments as recorders of glaciated and ice-free conditions have been limited to middle and high latitudes. This investigation interprets the paleoclimatic record preserved in the clastic sediments of a low latitude proglacial lake, Lake Caserococha, Peru.

The glaciolacustrine sediments of Lake Caserococha can be divided into three distinct lithologic sections: an upper, homogeneous, organic-rich section; a middle, banded section of clays and silts; and a lower inorganic section of till, including particles of all sizes.

Using visual examination of the core, smear slide sampling and analysis, and X-ray diffraction sampling and analysis, it is possible to observe various changes in sediment characteristics downcore. These changes suggest that the boundary between the lower till section and the middle banded section probably marks the time when the ice receded from the lake. However, the ice remained nearby within the lake's drainage basin, and controlled the sediment deposition of the lake for an additional period in which the banded section was deposited. The boundary between the middle, banded section and the upper, homogeneous section marks the time when there was a loss of major nearby glacial input. This change in lithologies from ice-controlled deposition to deposition that is not ice-controlled suggests the date of deglaciation of the region surrounding Lake Caserococha to be approximately 12,000 y.b.p.

The laminae of the banded section located between 290 cm and 500 cm downcore, suggest the presence of seasonal varves, each with inverse proportions of clay to biogenic abundance; however, a few of the laminae may represent storm deposits.

TABLE OF CONTENTS

LIST OF ILLUSTRATIONS AND TABLE

ACKNOWLEDGEMENTS

The author wishes to acknowledge several individuals who were instrumental in providing assistance for completion of the laboratory investigation and writing this paper. Highest gratitude is extended to Dr. Lawrence Krissek, Department of Geology and Mineralogy, who developed the idea for the investigation and sparked the author's interest in the sediment analysis. Dr. Krissek generously gave his time to discuss the problem and to provide instruction for laboratory methods. His patience and generosity are much-appreciated.

Dr. Paul Colinvaux was most generous in giving permission to use the sediment core and providing laboratory facilities for sampling. Dr. Rodney Tettenhorst assisted with X-ray diffraction procedures. Paul Heisig and Phil Hughes were helpful in providing assistance with laboratory procedures. Gratitude is also extended to Patricia Wackler, who typed the final draft, and to Glenn Knopf for helpful suggestions and assistance in writing the paper.

INTRODUCTION

A primary purpose of the investigation of sediments in glacially-influenced environments is to obtain a record of climatic fluctuations. Glaciolacustrine sediments, which are deposited continuously in freshwater lakes of glacial origin, usually remain undisturbed for many thousands of years. As a result, these deposits yield a continous paleoclimatic record.

Traditionally, such paleoclimatic studies have utilized data on the abundance, composition, and variations of warm and cold temperature pollen assemblages through time (Colinvaux, 1972). Other studies have been performed on the stratigraphy, composition, and aerial distribution of glacial tills, moraines, and glaciolacustrine sediments (Ashley, 1975; Ludlam, 1979; Rymer and Sims, 1982; van der Hammen, 1978). Pollen assemblages have been studied in glacially-influenced environments from low to high latitudes, but studies of clastic sediments as recorders of glaciated and ice-free conditions have been limited to middle and high latitudes.

This investigation of the glaciolacustrine sediments of Lake Caserococha, Peru, is designed to identify and interpret the paleoclimatic record preserved in the sediments of this low-latitude glacial system. This objective will be achieved by relating large-scale, visually-identifiable sediment characteristics to compositional characteristics in order to evaluate the processes and sediment sources controlling deposition. Specifically, the sediment will be examined to determine the compositional differences controlling variations in sediment appearance. In addition, the investigation will attempt to determine which sediment characteristics, grain size, composition (biogenic to non-biogenic material), and massive vs. layered structure, are the most

consistent indicators of glacial influence. Variations in these consistent glacial indicators will be examined to determine if the sedimentary record at Lake Caserococha is sensitive to minor climatic fluctuations.

This investigation carefully examines a sedimentary sequence that was deposited during a period of major and minor climatic fluctuations. The sediment was deposited in the vicinity of a low-latitude alpine glacier. The core was taken by Dr. Paul Colinvaux, Deparment of Zoology, The Ohio State University, in June, 1977, from Lake Caserococha. The lake, located on the eastern slopes of the Peruvian Andes at approximately $13^{o}38'S$, $71^{o}17'W$, and an elevation of 3900 meters, is a small, approximately 0.3 km x 0.2 km, proglacial lake.

The core was recovered from the center of the lake at a water depth of 5.5 meters, and the sedimentary section is approximately 750 cm in length. A preliminary description of the gross sediment characteristics and available age data in ^{14}C y.b.p. are shown in Figure 1 (Colinvaux, 1983, unpublished). The date of 15,330 $\pm$ 210 y.b.p. at the interval 439 to 459 cm suggests that these sediments span the end of the last glacial maximum and extend through the post-glacial to the present. For this reason, this core appears to provide a suitable record for the investigation of sedimentary response to changing environmental conditions in a low-latitude glacial system.

The three major sediment types described by Colinvaux--gray, pebbly clay; banded silts and clays; and brown gyttja (Figure 1)--will be examined for variations both within and between lithologies. Analyses within the banded section will be emphasized, in order to determine the importance of the banding as a response to depositional conditions.

LAKE CASEROCOCHA CORE

PRELIMINARY LOG

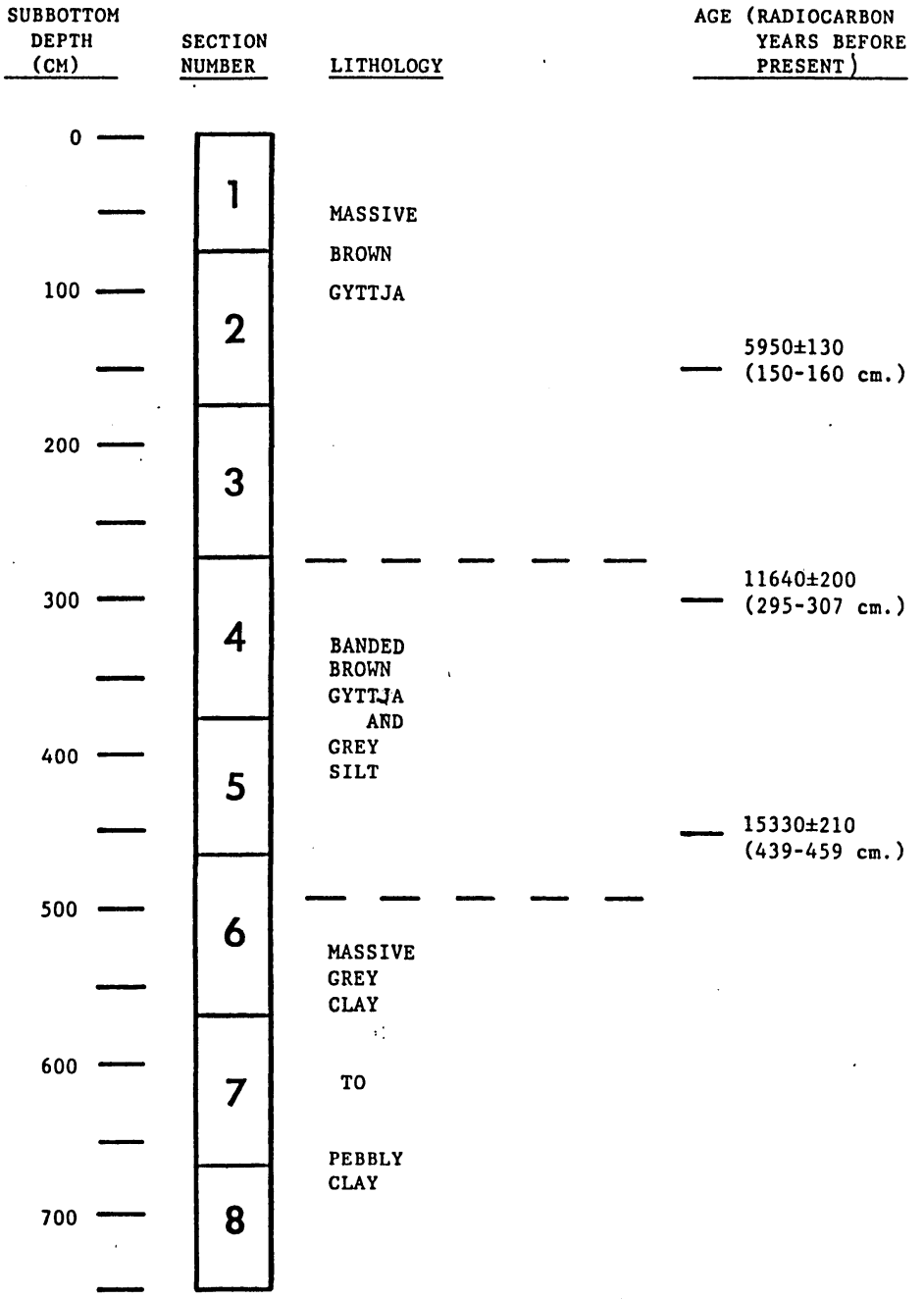

Figure 1

PROCEDURE

The procedure of the analysis of the glaciolacustrine sediments of Lake Caserococha, Peru, was a laboratory investigation that consisted primarily of three parts: development of a core log, smear slide sampling and analysis, and X-ray diffraction sampling and analysis.

Core Log

In the first stage of this study, the 7½ meter core, encased in eight 1 meter aluminum sections, was examined to develop a core log. The core log describes general sediment characteristics within the core, such as color (relative to a Munsell soil color chart), structure, and grain size. Sample locations were also recorded (Appendix I). A general core description was based upon visual observation and examination of X-radiographs. The X-radiographs were useful because they showed light and dark laminations that were not obvious in visual observation. In addition, the X-radiographs indicated potential locations for sampling the laminated sections, and provided an accurate measure of initial core length. Subsequent shrinkage because of drying has affected the cores since the X-radiographs were taken.

Smear Slide Analysis

Very small smear slide samples were taken and smeared onto slides using a toothpick. Histological mounting medium was then applied beneath a coverslip, and slides were heated to harden the mounting medium.

Smear slides were examined using a petrographic microscope to determine relative percentages of the various constituents. Six major constituents--plant material, diatoms, clay, ash, quartz and accessory minerals, and opaque minerals--were observed, and relative percentages of each sample's bulk composition were recorded in tabular form (Appendix II).

X-ray Diffraction Analysis

Sediment samples of approximately 5 cc were taken from various depths downcore for preparation of slides for X-ray diffraction analysis (locations are shown in the Core Logs, Figures 2 through 9). Each sample was treated with 30% hydrogen peroxide, H_2O_2, to destroy organic matter. The H_2O_2 was buffered with ammonium hydroxide, NH_4OH, to preserve carbonates. Following destruction of the organics, when the addition of excess H_2O_2 solution to the sediment no longer produced a reaction, the sediment was sieved at 63μm, separating the sand-sized and larger fraction from the silt and clay-sized fraction.

The less than 2μm fraction was then separated from the silt and clay mixture by settling and decantation. The settling was repeated twice for each sample to promote a more complete separation. The decanted portion of the solution, which contained particles 2μm and smaller, was collected and centrifuged to concentrate the clays. The concentrated suspension was then repeatedly applied to glass slides until a thick, even coat of oriented clay grains was obtained (four to five applications until the sediment slide was no longer transparent). The slides were put into an ethylene-glycol dessicator in a 60^{o} oven overnight to expand the smectites. The slides were then X-rayed on the Department of Geology and Mineralogy Philips X-ray diffraction system at 2^{o}/minute, 60"/hour, 3^{o} to 30^{o} 2θ, 500 counts full scale, and Cu Kα radiation, in order to determine the abundances of chlorite and illite.

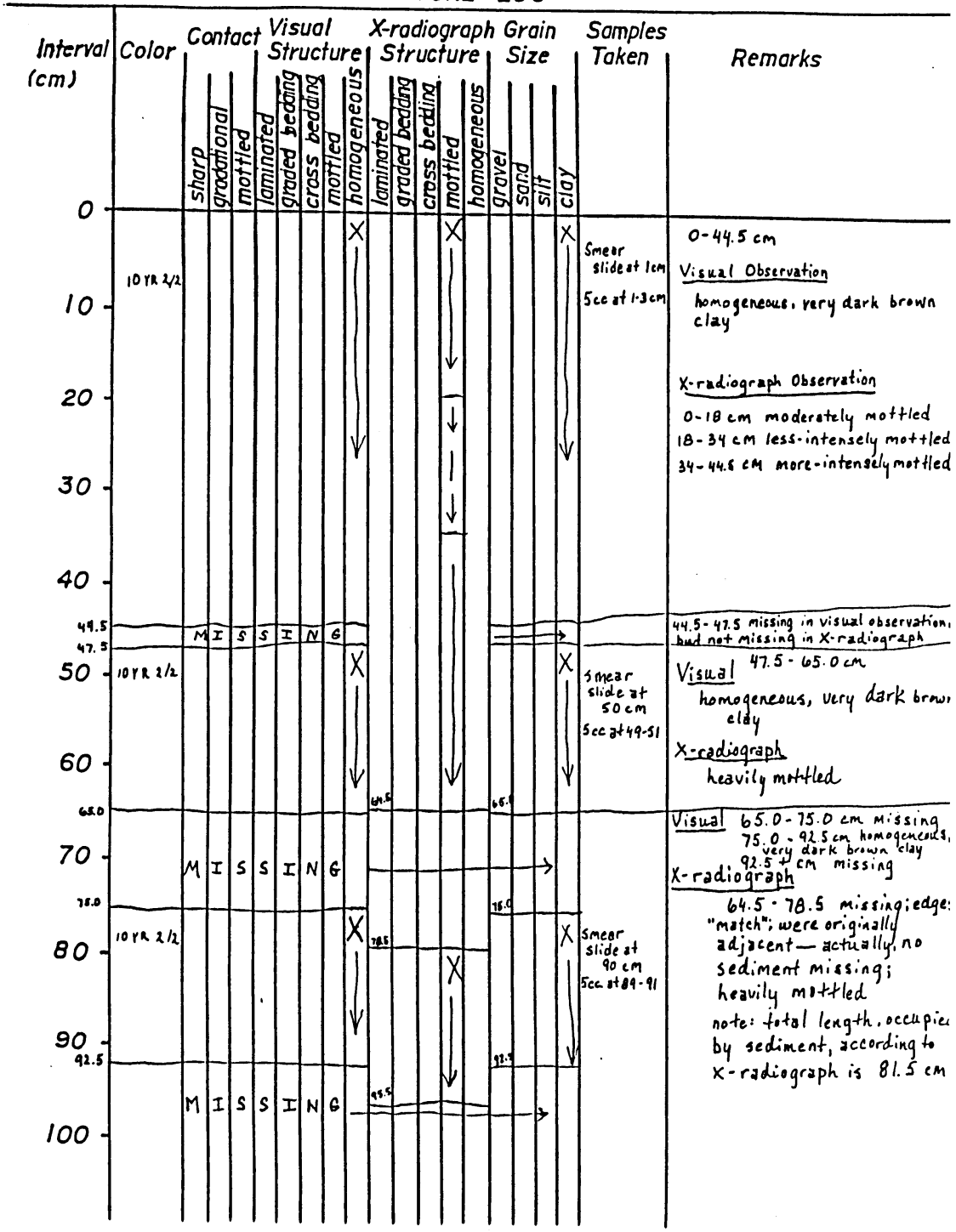

Figure 2: Core Log Section 1

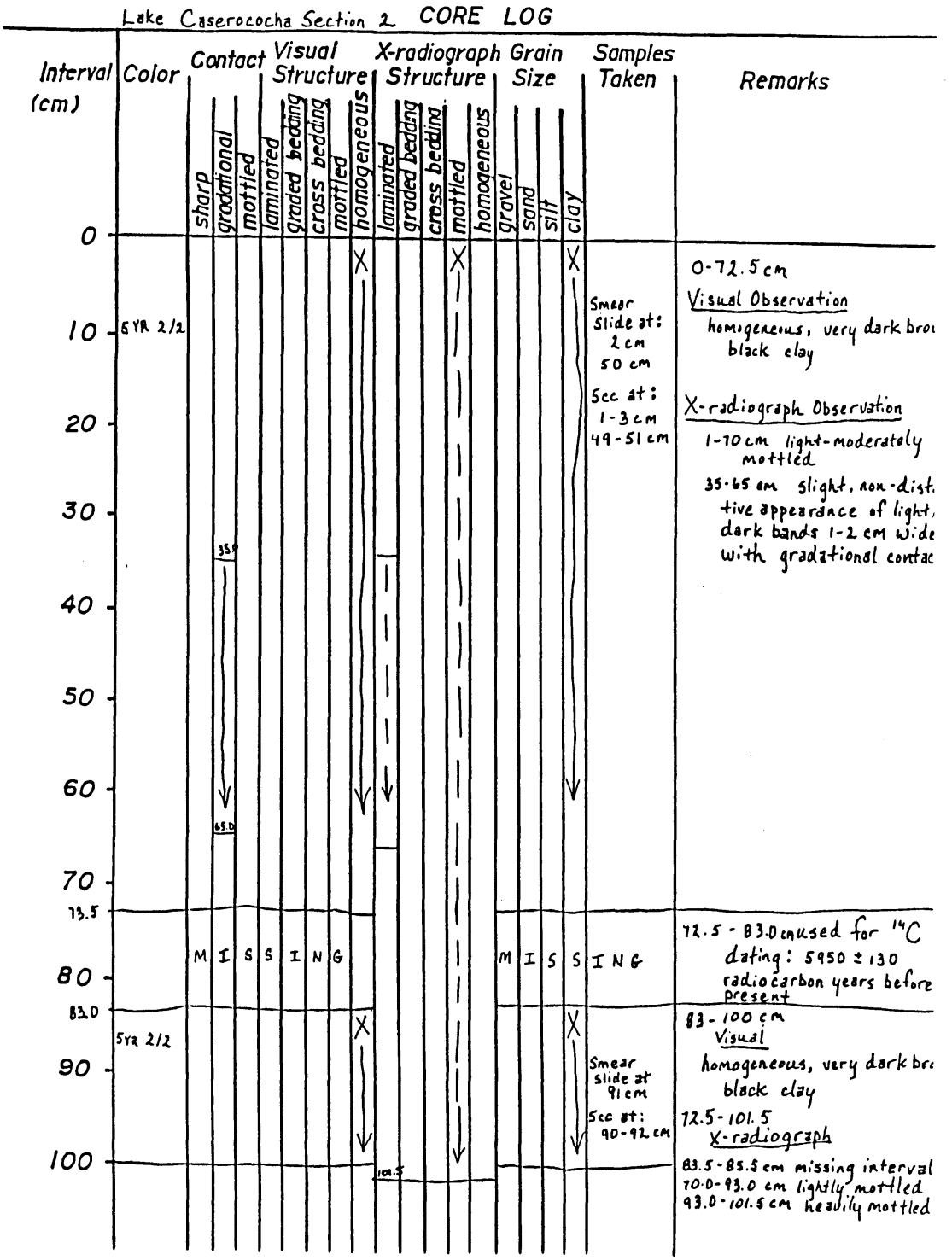

Figure 3: Core Log Section 2

Lake Caserococha Section 3 CORE LOG

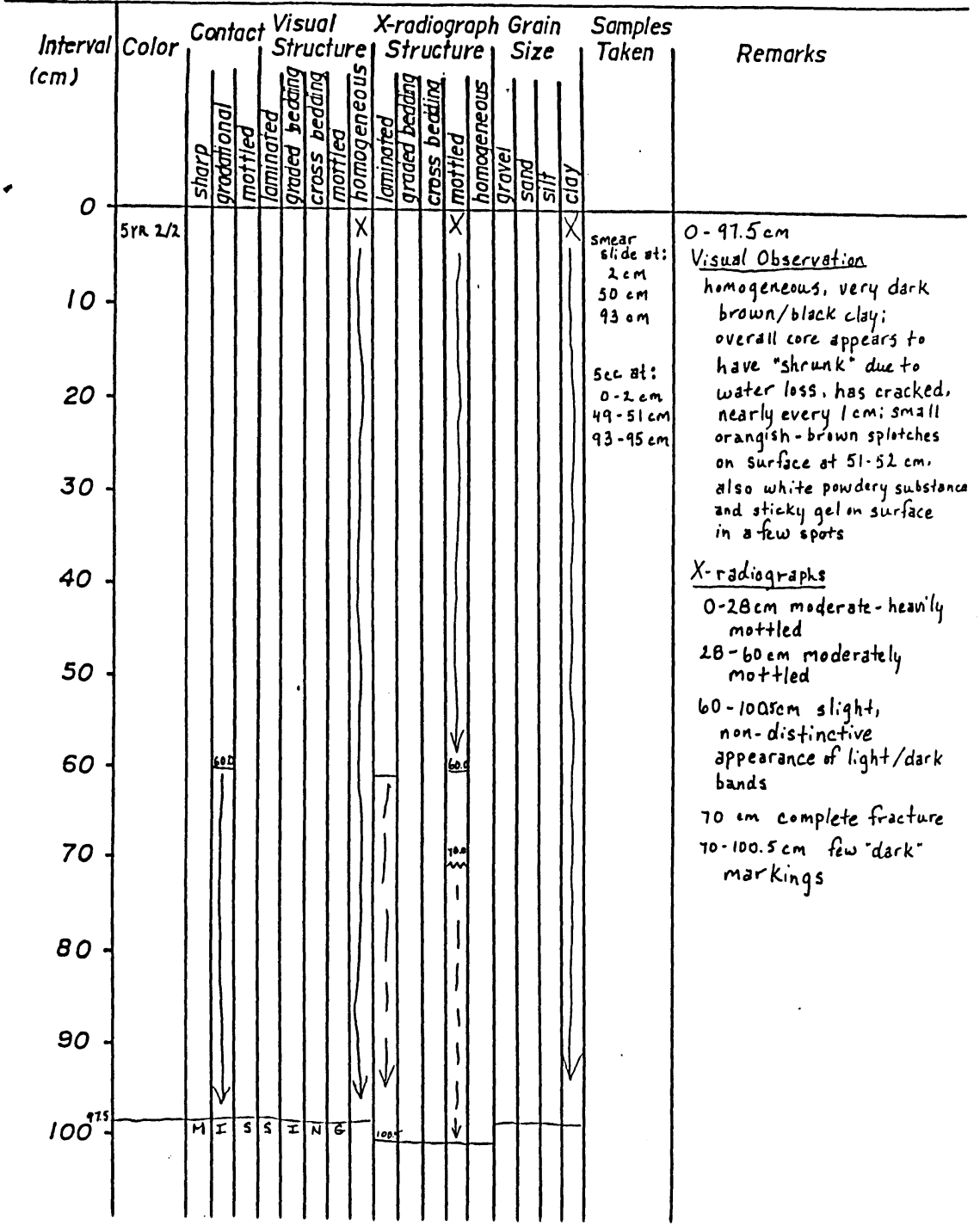

Figure 4: Core Log Section 3

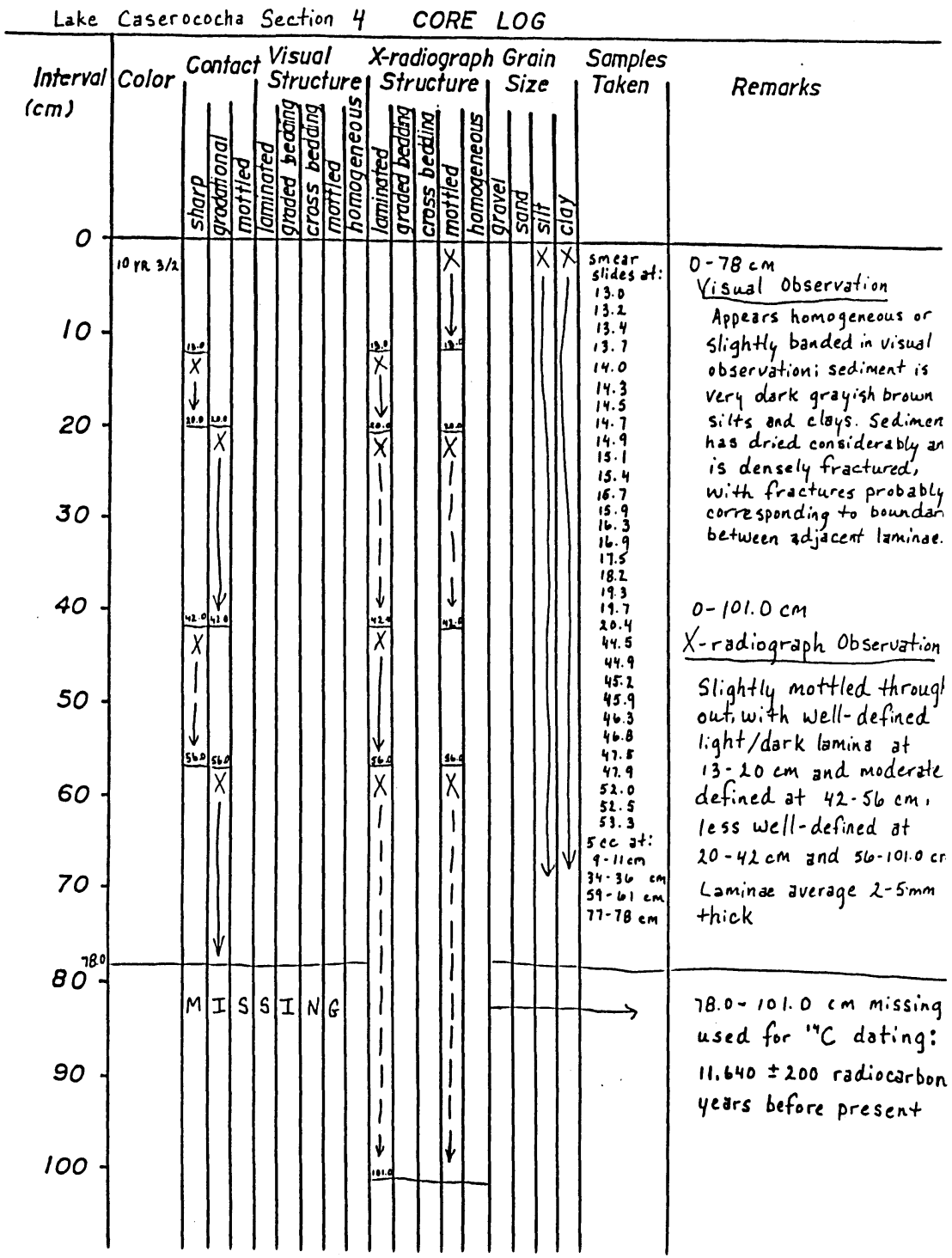

Figure 5: Core Log Section 4

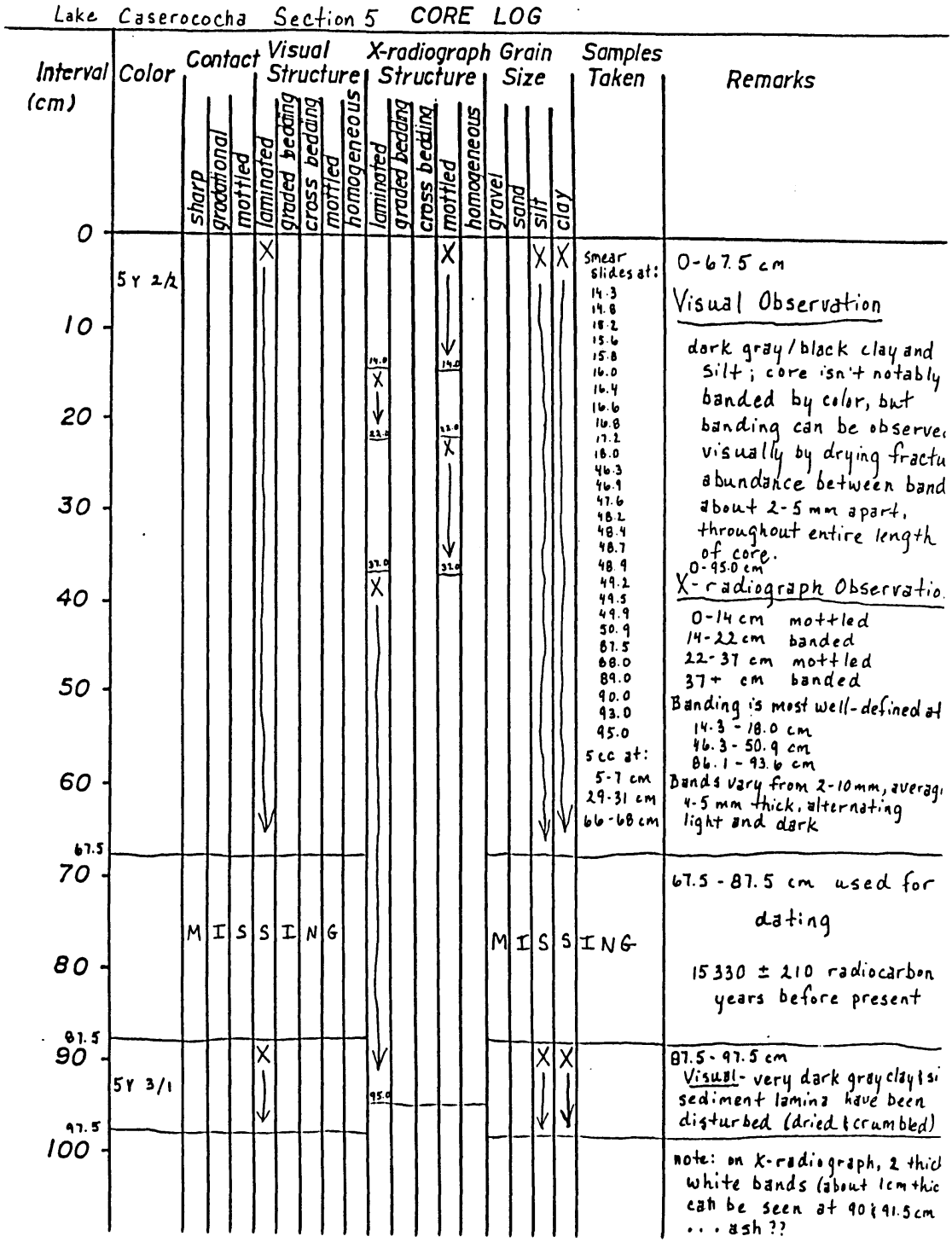

Figure 6: Core Log Section 5

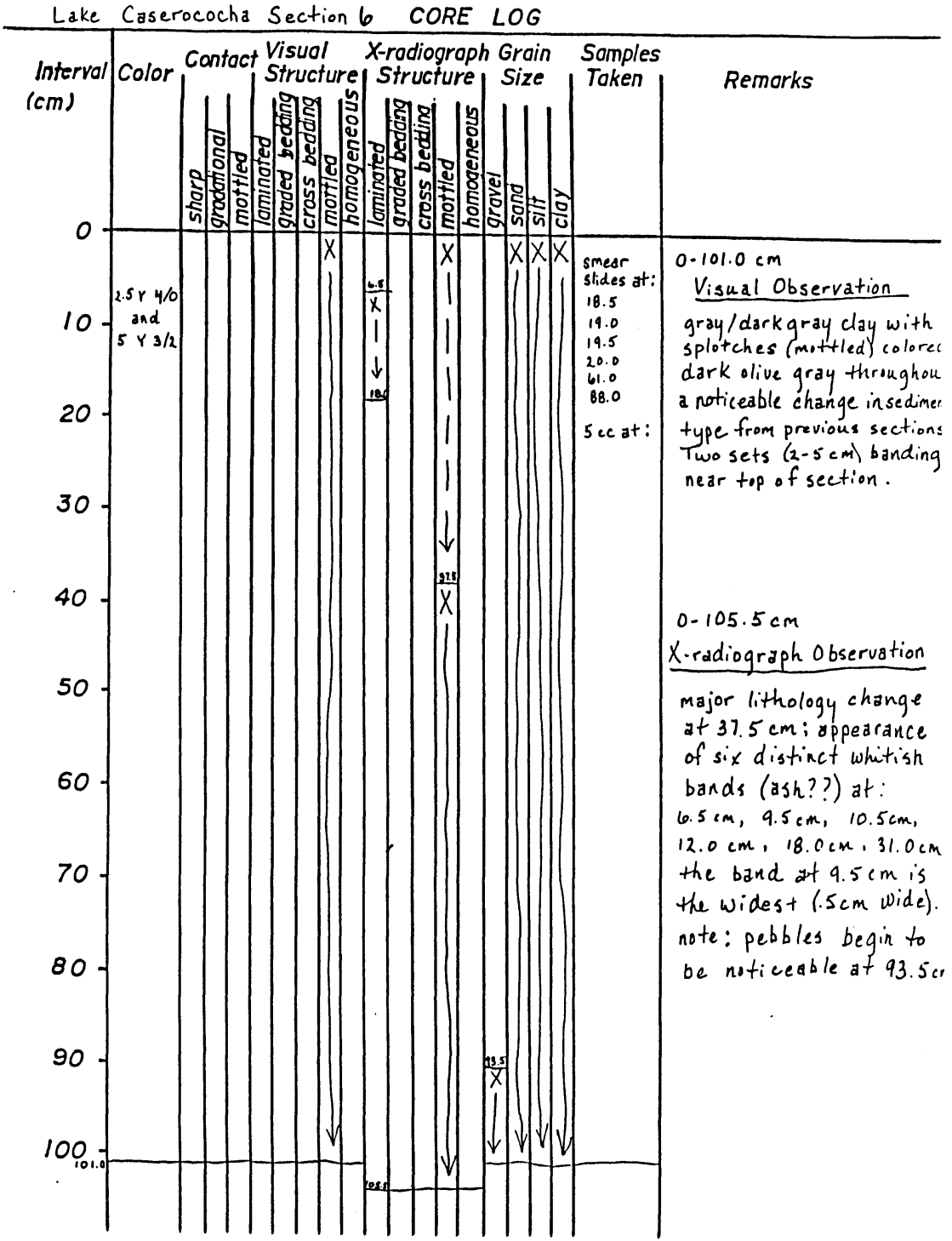

Figure 7: Core Log Section 6

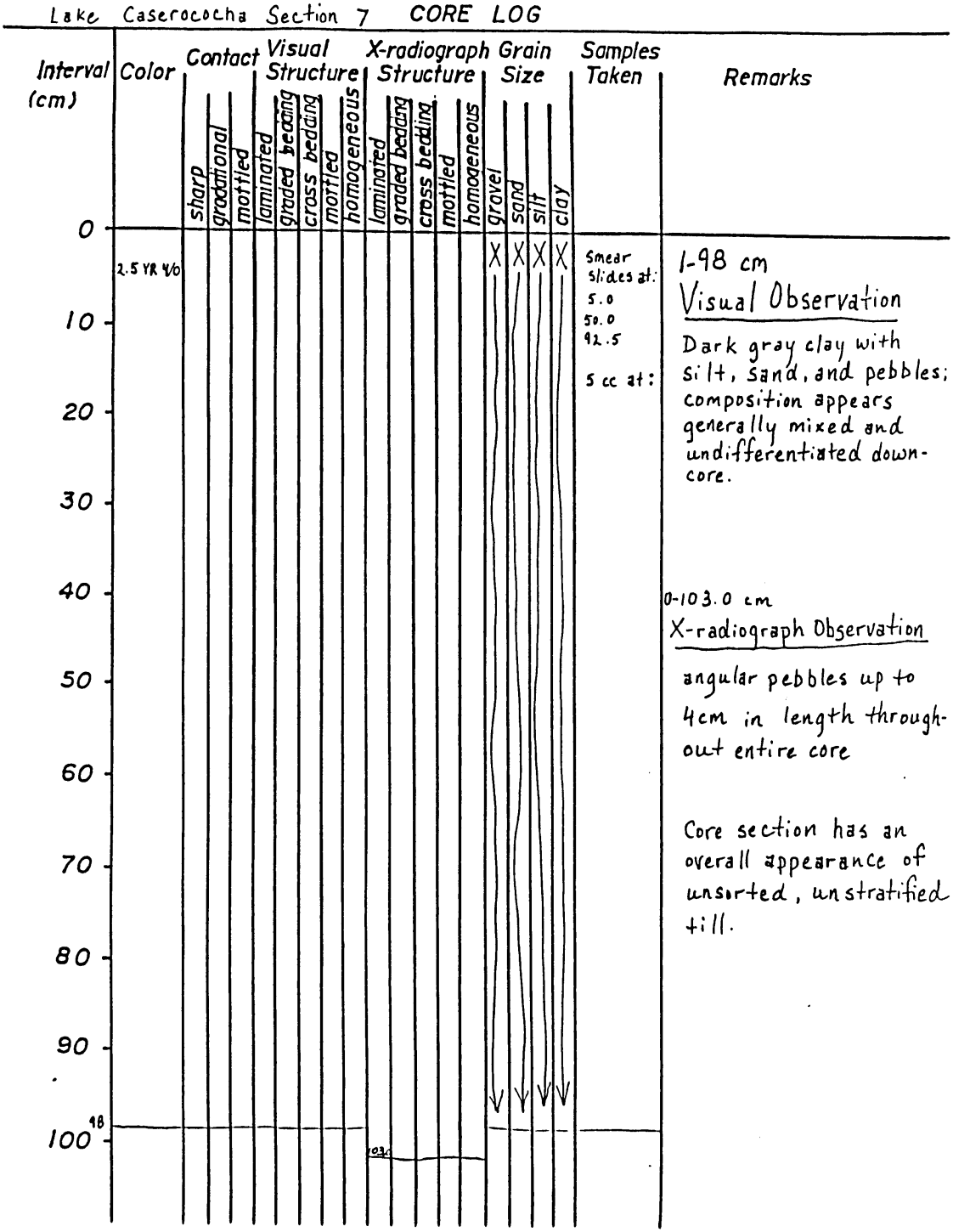

Figure 8: Core Log Section 7

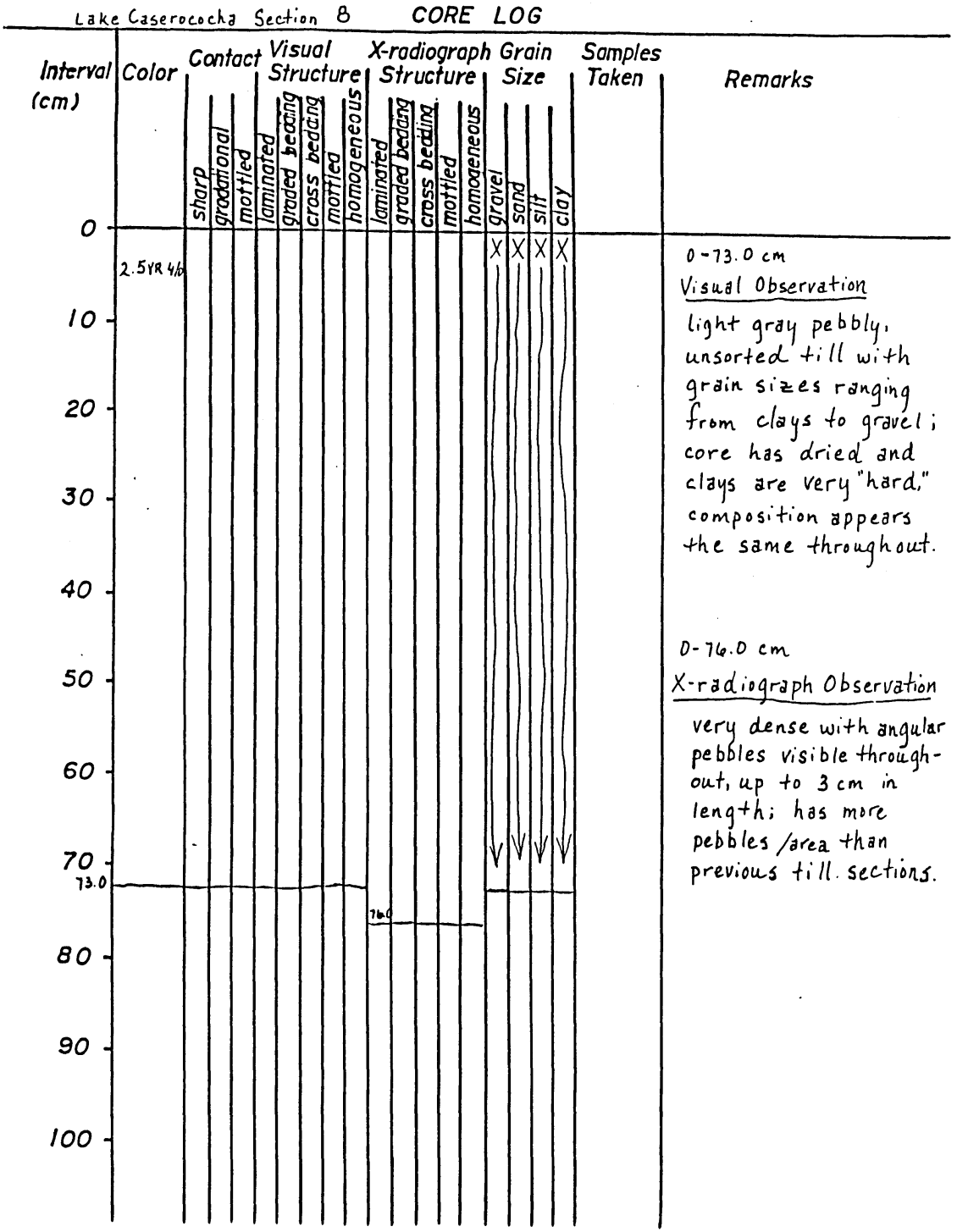

Figure 9: Core Log Section 8

DATA

Core Logs

Each 1 meter section of the $7\frac{1}{2}$ meter core was measured and described in a core log. Section one, which measures 92.5 cm long in visual observation and 95.5 cm long on the X-radiograph, has a gap of 14.0 cm with no sediment (Figure 2). On the X-radiograph, the sediments on each side of the gap appear similar, and the boundaries of the two blocks fit together well. As a result, the gap is interpreted to mark a place where the sediment core separated when the sediment "slid" within the section, probably during its removal from the lake. The true section length, as measured on the X-radiograph, is 81.5 cm. The section is a homogeneous, very dark brown clay, and appears to be mottled on the X-radiograph.

Section two measures 101.5 cm on the X-radiograph and 100.0 cm in visual observation, with probable shrinkage of 1.5 cm since the X-radiograph was made (Figure 3). The interval of 72.5 cm to 83.0 cm deep was radiocarbon-dated at 5950 $\pm$ 130 y.b.p., and is presently missing from the core. Section two is nearly identical to section one, and is a homogeneous, very dark brown/black clay. From 35.0 cm to 65.0 cm deep, faint light and dark bands one or two centimeters wide appear on the X-radiograph. However, these bands are not as well developed as those found in sections four, five, and six.

Section three sediment, also a homogeneous very dark brown/black clay, exhibits drying and shrinking (Figure 4). The X-radiograph reveals a moderately to heavily mottled appearance with faint banding from 60.0 cm to 100.5 cm

Section four shows a noticeable change in lithology from the upper three sections (Figure 5). In this section, the sediment consists of very dark grayish brown silts and clays. Section four has also dried and is densely fractured, with the fractures probably corresponding to boundaries between adjacent laminae. The laminated nature of section four is obvious on the

X-radiograph. The laminae are best-defined in intervals from 13.0 cm to 20.0 cm and 42.0 cm to 56.0 cm, and are less well-defined from 20.0 cm to 42.0 cm and 56.0 cm to 101.0 cm, with the laminae averaging two to five millimeters thick through all banded intervals. The horizon from 78.0 cm to 101.0 cm was used for radiocarbon dating, and is dated at 11,640 $\pm$ 200 ^{14}C y.b.p.

Section five is composed of dark gray/black clay and silt, with fractures approximately two to five millimeters apart, located between bands throughout the section (Figure 6). Section five measures 95.0 cm on the X-radiograph, and shows well-developed banding at three levels, with bands ranging from two to ten millimeters thick and averaging four or five millimeters thick. Banding is best defined from 14.3 cm to 18.0 cm, 46.3 cm to 50.9 cm, and 86.0 cm to 93.6 cm, with a mottled appearance elsewhere. The interval from 67.5 cm to 87.5 cm has been radiocarbon-dated at 15,330 $\pm$ 210 y.b.p., suggesting that the level of the globally-recognized last glacial maximum occurs close to this depth. On the X-radiograph, two one-centimeter thick white bands are located at 90.0 cm and 91.5 cm, and probably represent volcanic ashes. The section is disturbed, dried and crumbled between 87.5 cm and 97.5 cm.

Section six exhibits a different color than the upper five sections, being silvery gray with dark olive gray splotches throughout (Figure 7). Section six is 105.5 cm long, with pebbles occurring from 93.5 cm to the bottom. Clay is mixed with silt and fine sand throughout the section. In the X-radiograph, the lithology of core six exhibits a noticeable change at 37.5 cm. Six distinct, whitish bands, each of which probably represents a a volcanic ash, are apparent at 6.5 cm, 9.5 cm, 10.5 cm, 12.0 cm, 18.0 cm,

and 31.0 cm. The band at 9.5 cm is the widest of the six being 0.5 cm in width.

Section seven is a dark gray clay with silt, sand, and pebbles found throughout the core (Figure 8). The composition of core seven appears generally mixed and undifferentiated down section. The section measures 103.0 cm long on the X-radiograph, with angular pebbles up to four centimeters in length occurring throughout its entirety. The general appearance of core seven suggests an interpretation as an unsorted, unstratified till.

Section eight, which is similar to section seven, is a pebbly, unsorted till, with grain sizes ranging from clays to gravel. The textural composition of section eight appears uniform throughout its length (Figure 9). The core has dried and the sediment is very hard, making it difficult to sample. On the X-radiograph, section eight appears very dense, with angular pebbles up to three cm in length. This section also contains more pebbles than section seven.

Average Composition Throughout the Core

On the basis of general sediment characteristics, samples from the Lake Caserococha core were subdivided into eight stratigraphic groups. Each group, however, does not necessarily correspond to one particular section of the core; for example, set 8 contains samples from the sixth, seventh, and eighth meters of the core. These groups represent either large-scale, uniform intervals within the core, or detailed sets of samples from adjacent laminae within the banded sections of the core. The samples contained within each group are listed in Table 1, which also presents the average composition of each of the four main constituents within each of the eight sets of samples.

Table 1: Average Composition of Eight Sets of Samples

Set #	Depth Interval of Set (cm)	# of Samples in Set	Biogenous Material (%)	Clay (%)	Ash (%)	Quartz & Accessory Minerals (%)
1	0-276.0	9	50	45	2	3
2	296.5-303.9	20	40	37	5	18
3	328.0-336.8	11	48	41	3	8
4	398.8-402.5	11	28	57	4	11
5	430.8-435.4	11	35	52	5	8
6	472.0-479.5	6	13	56	27	4
7	498.0-499.5	4	3	53	40	4
8	540.5-753.0	7	0	49	18	33

These constituents are: biogeneous material (including plant material and diatoms), clay, ash, and quartz and accessory minerals. (See Appendix II for initial data).

As indicated in Table 1, the upper three sample sets contain relatively more biogeneous material than the lower five sample sets. The abundance of biogenics ranges from 50% to 0% from the top to the bottom of the core.

The amount of clay present is essentially constant throughout the core, with non-systematic fluctuations from 37% to 57%. No general pattern of increasing or decreasing clay content occurs downcore. In contrast, the ash content increases downcore, with the highest average, 40%, in the seventh set of samples (498.0 cm to 499.5 cm).

The abundance of quartz and accessory minerals varies from 3% in set 1 to 33% in set 8, with several fluctuations in between.

Triangle Plots: Comparative Abundances of Three Constituents

Triangle plots are useful for comparison of relative abundances of a combination of three major constituents in each sample. The following three illustrations are based upon the compositional abundances of all major components of these samples, as determined by smear slide analysis (tables of bulk composition are provided in Appendix II). The eight sets of samples discussed here are the eight sets mentioned previously (Table 1).

In Figures 10-a and 10-b, the three major components compared are biogenics, quartz and accessory minerals, and ash. Sets 1 through 5 show a high biogenic content compared to the lower three sets, while sets 6 through 8 contain relatively more ash than sets 1 through 5. All sets show similar low percentages of quartz, except for set 8, which has more than 50% quartz and accessory minerals.

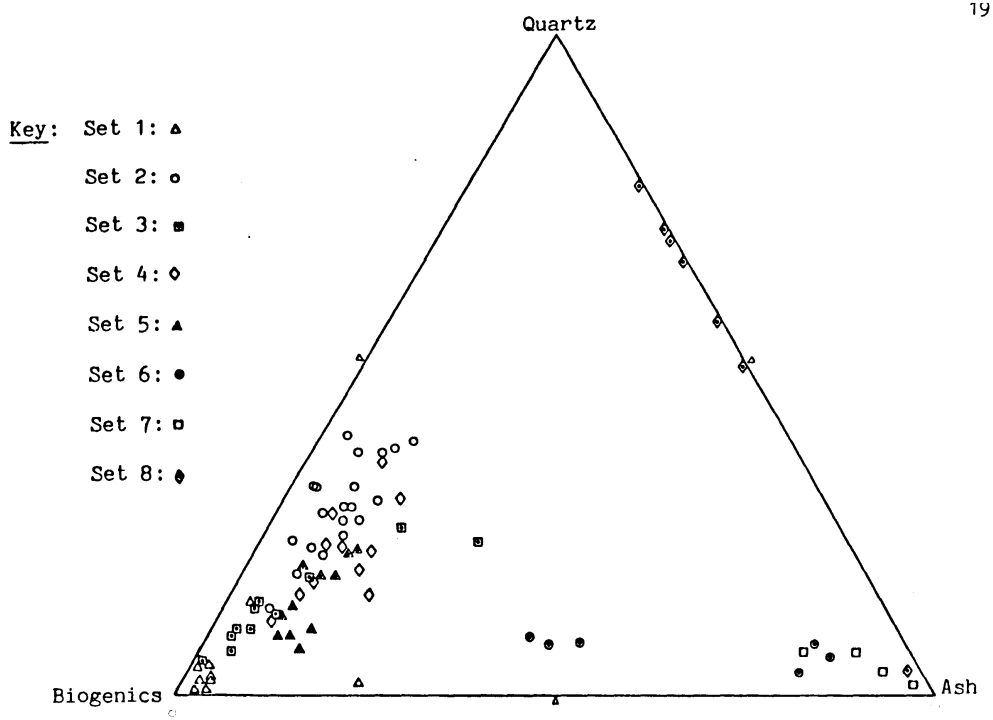

Figure 10-a
Triangular Plot Comparing Quartz, Ash, & Biogenic Abundances

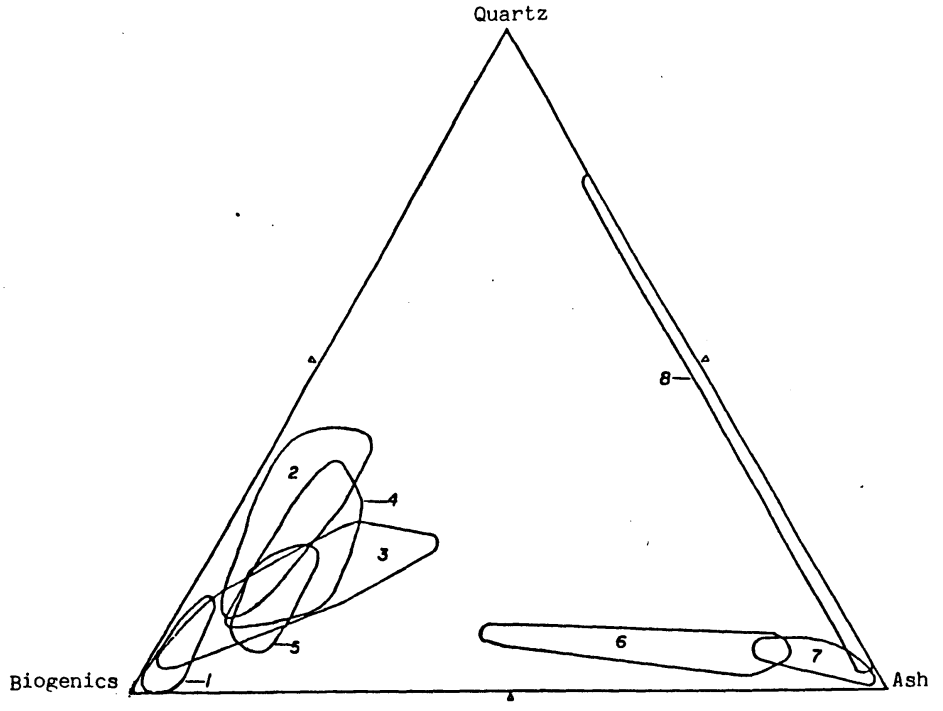

Figure 10-b
Triangular Plot Comparing Quartz, Ash, & Biogenic Abundances

Biogenics, clay, and ash abundances are compared in Figures 11-a and 11-b. A notable difference in biogenic abundance downcore can be observed because most samples in sets 1 through 3 contain more than 50% biogenous material. The abundance of biogenics decreases progressively downcore in sets 4 through 8, with no biogenics in set 8. Differences in clay abundance between the sets are not as obvious as changes in biogenic content. Clay abundance, however, does increase slightly in sets 6 through 8, particularly when compared with sets 1 through 3, which generally contain less than 50% clay. As described previously for Figures 10-a and 10-b, the abundance of ash shown in Figures 11-a and 11-b is rather low (near zero) in sets 1 through 5. Ash abundance is as high as 50% in sets 6 through 8.

Additional and valuable distinctions can be made between samples by comparing their quartz, clay, and biogenic contents. Three groups of samples can be identified in Figures 12-a and 12-b, based upon their biogenic material content. Sets 1 through 3 have a relatively high percentage of biogenics, often with more than 50% biogenics in each set. Sets 4 and 5 show a gradual decrease in abundance of biogenics, approaching the relatively low contents in sets 6 through 8. No biogenics are present in most of set 8. The abundance of clay varies inversely with the amount of biogenous material and increases downcore, with sets 6 through 8 containing a high abundance of clay. Set 7 is almost entirely clay. As previously indicated in Figures 10-a and 10-b, quartz is most prevalent in set 8.

Downcore Abundances of Four Major Sediment Constituents

While triangle plots provide information on characteristics of groups of samples from the Lake Caserococha core, supplemental information can be obtained by examining the detailed abundances of individual constituents

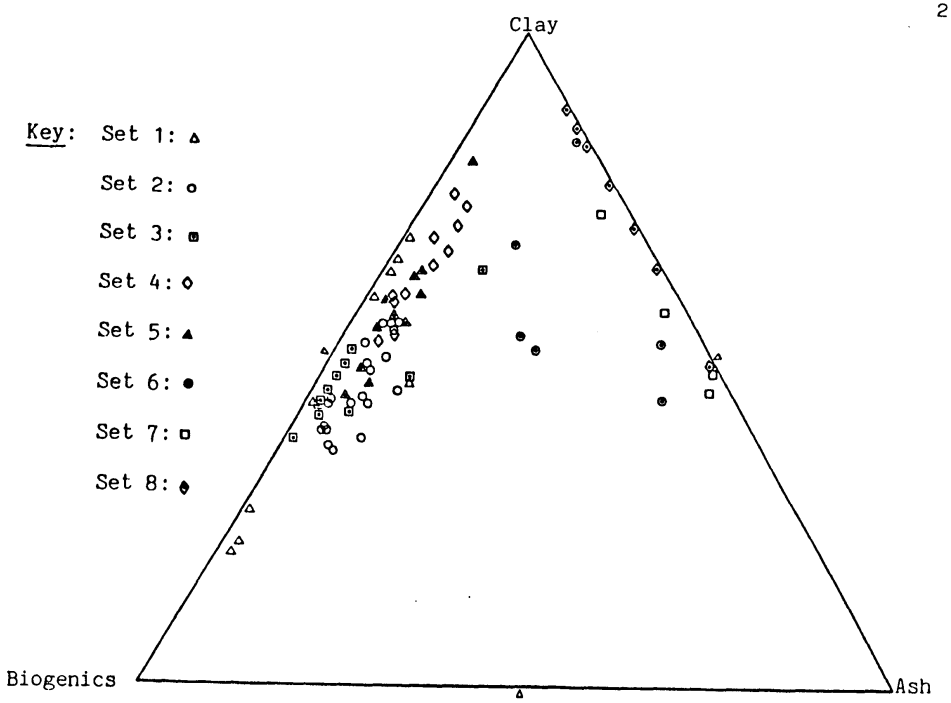

Figure 11-a
Triangular Plot Comparing Clay, Ash, & Biogenic Abundances

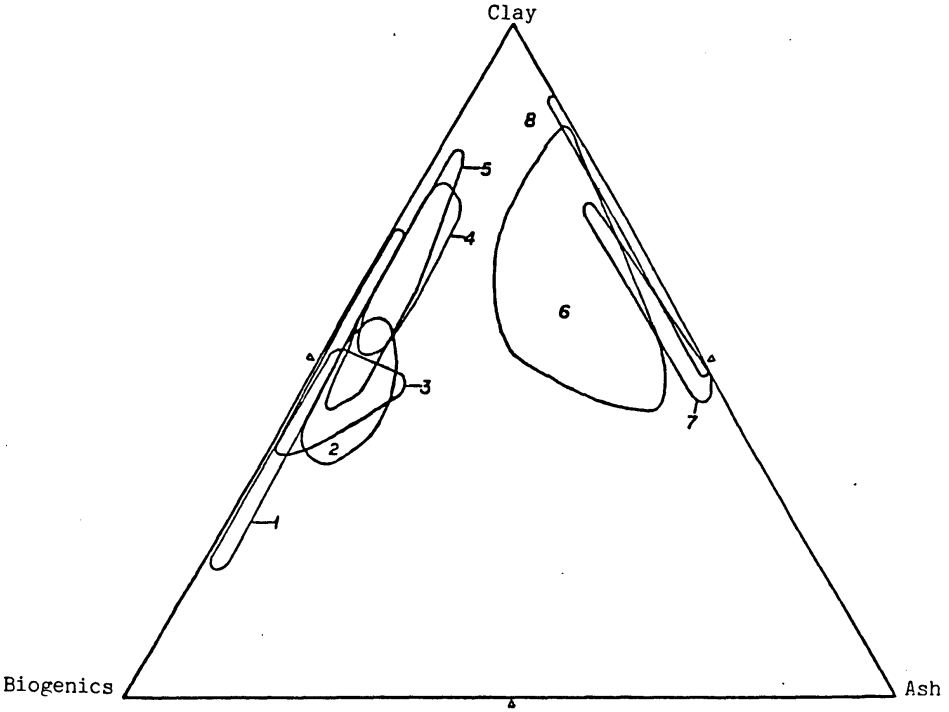

Figure 11-b
Triangular Plot Comparing Clay, Ash, & Biogenic Abundances

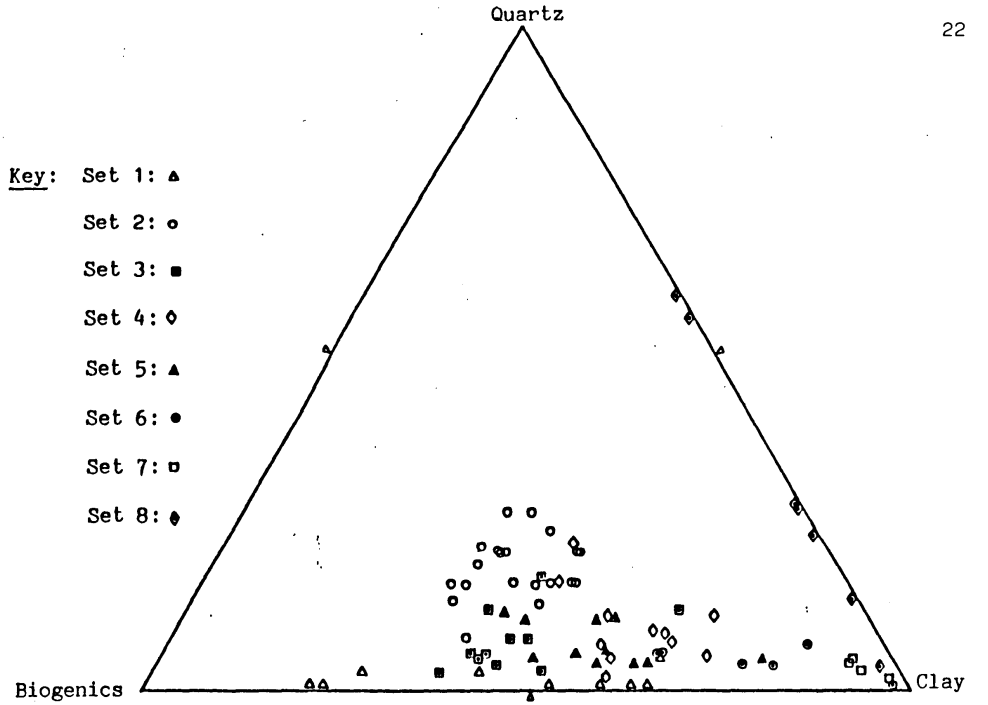

Figure 12-a
Triangular Plot Comparing Quartz, Clay, & Biogenic Abundances

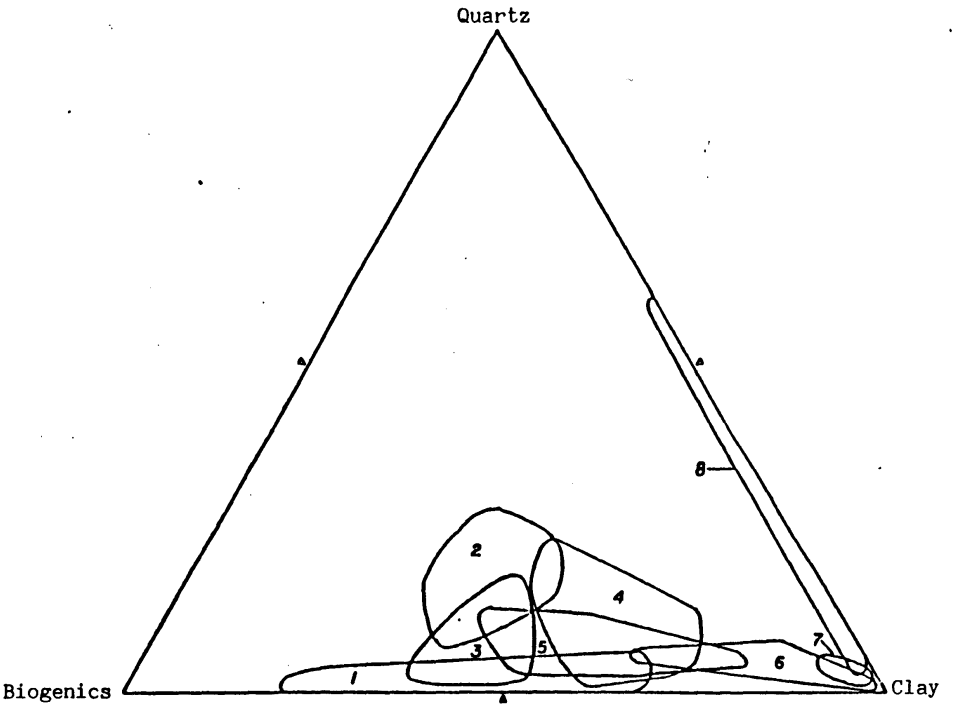

Figure 12-b
Triangular Plot Comparing Quartz, Clay, & Biogenic Abundances

downcore. These data are presented as plots of "Component Abundance vs. Depth". These graphs, which mark both general trends of increasing or decreasing abundances and superimposed shorter-term fluctuations downcore, are based upon smear slide samples taken at various depths within the core (Appendix II). For the six banded sections that were sampled, set averages are plotted by using an "X" to mark the mean of all samples within the set, and a line to represent the percentage range within the set.

Figure 13 presents the distribution of ash content downcore. Ash content is nearly zero in the upper 290 cm of the Lake Caserococha core, remains low throughout much of the banded section, but increases rapidly between 480 cm and 500 cm. Below approximately 480 cm, ash content remains high into the lower third of the core, where it decreases and fluctuates below 550 cm.

Clay abundances are shown in Figure 14, with a general pattern of increasing clay abundance downcore, particularly in the banded section. Each set of samples within the banded section has a relatively broad percentage range of approximately 30% to 40%.

Figure 15 illustrates the progressive downcore decrease in the abundance of biogenous material. The bottom 300 cm are virtually devoid of biogenics.

The overall abundance of quartz and accessory minerals is shown in Figure 16; these components increase downcore. However, the quartz abundance decreases downcore within the middle banded section. The increase with depth observed in the bottom third of the core is relatively constant, with the lowest sample containing the highest percentage of quartz found in the Lake Caserococha core.

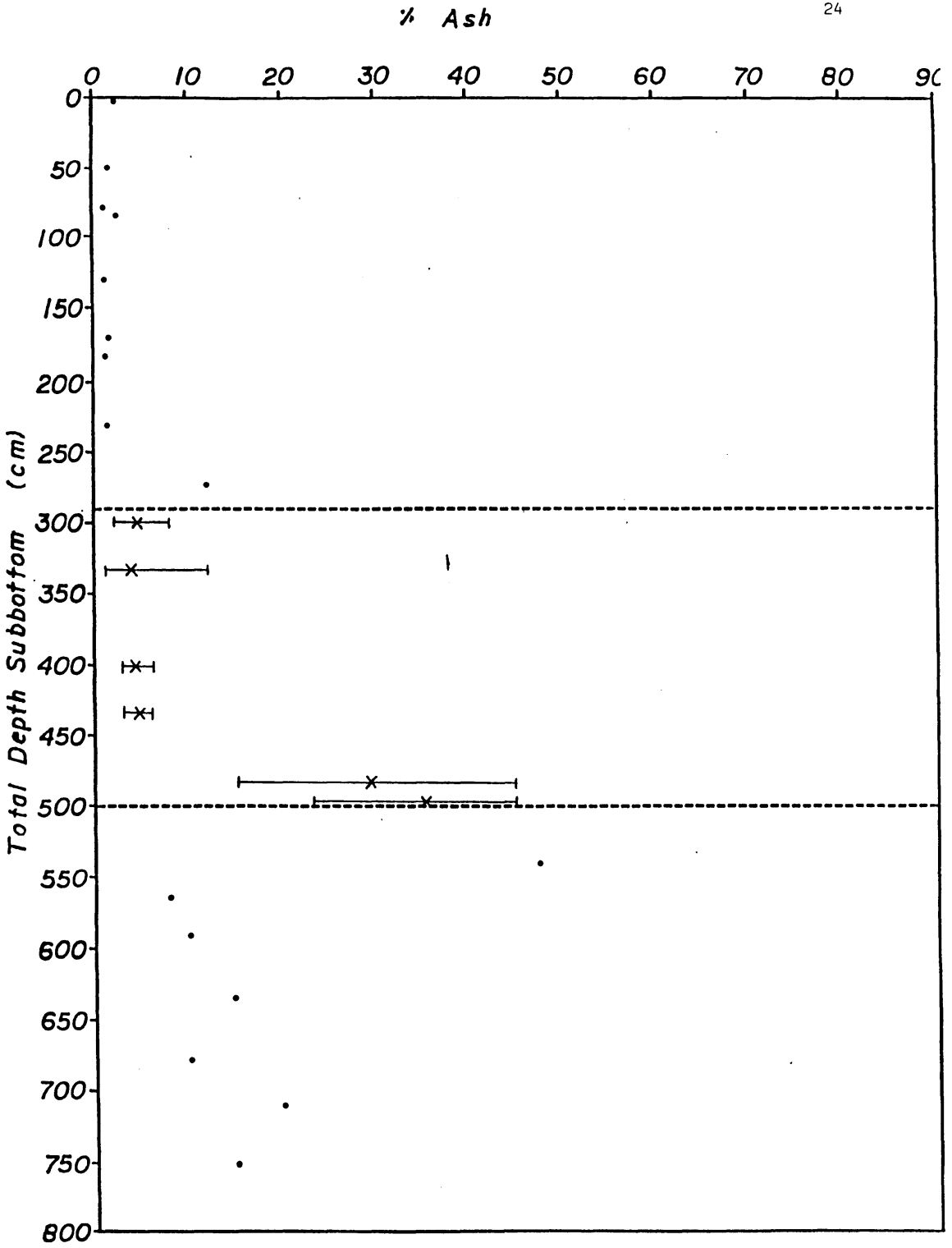

Figure 13: Ash Abundance (%) Downcore, Lake Caserococha

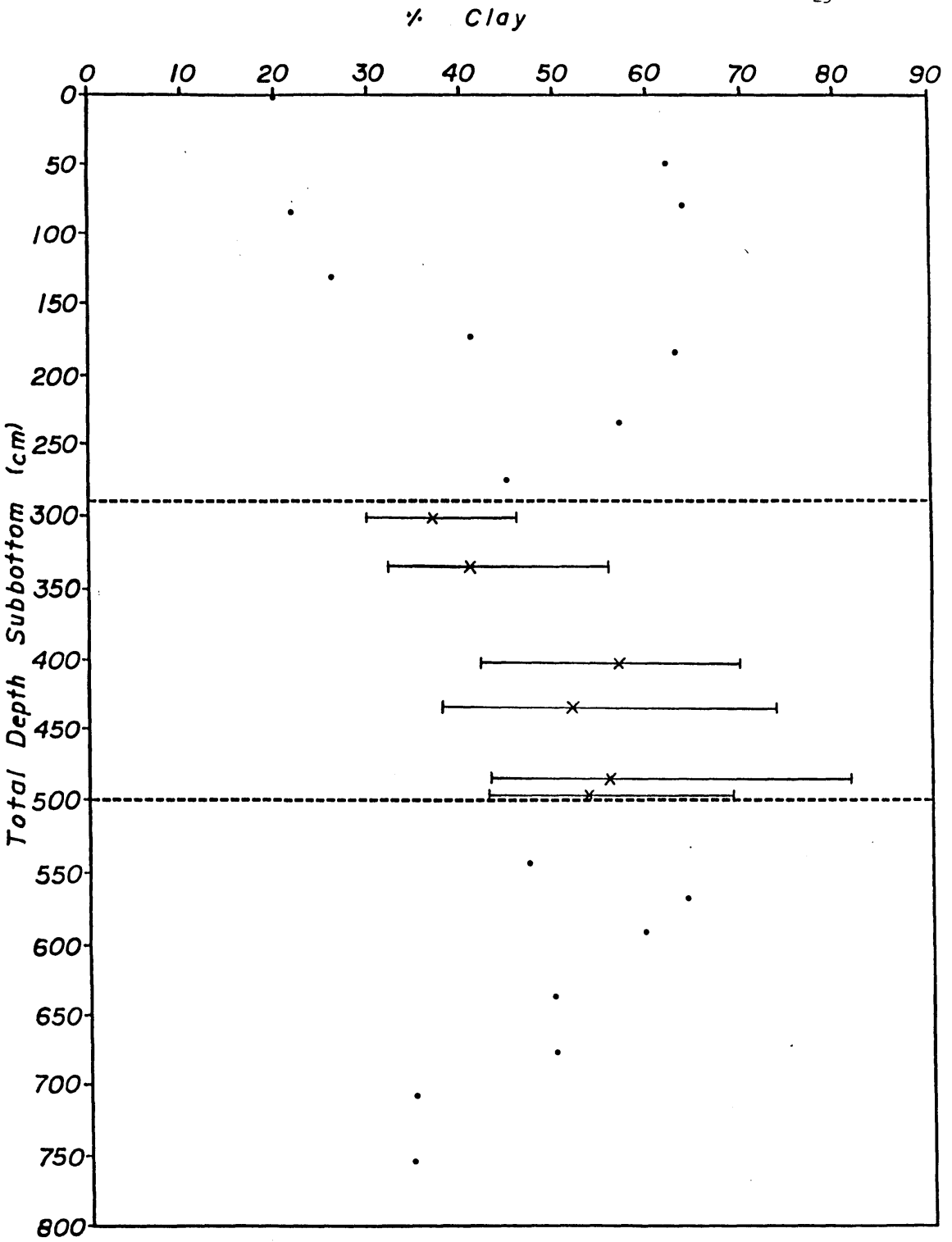

Figure 14: Clay Abundance (%) Downcore, Lake Caserococha

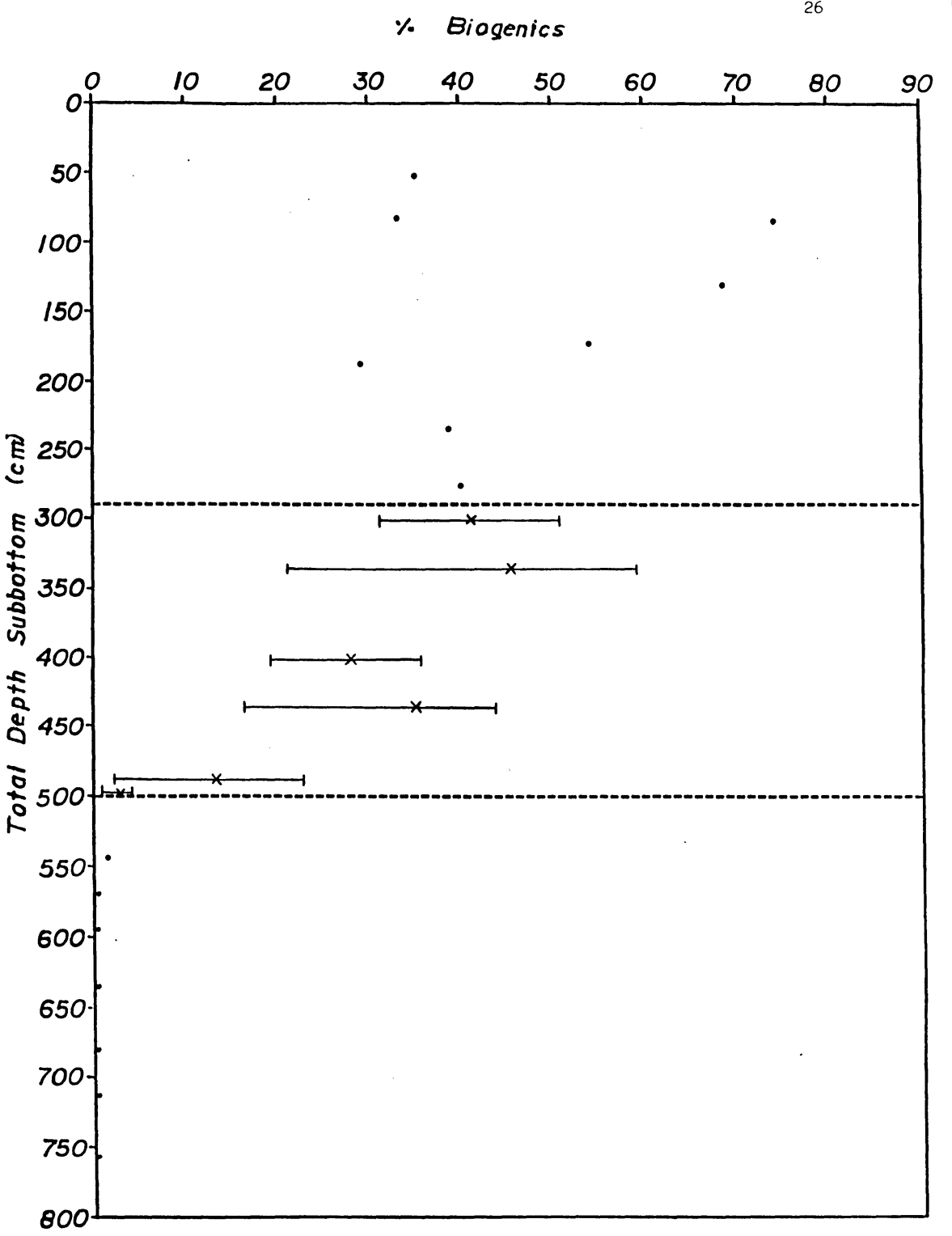

Figure 15: Biogenous Material Abundance (%) Downcore, Lake Caserococha

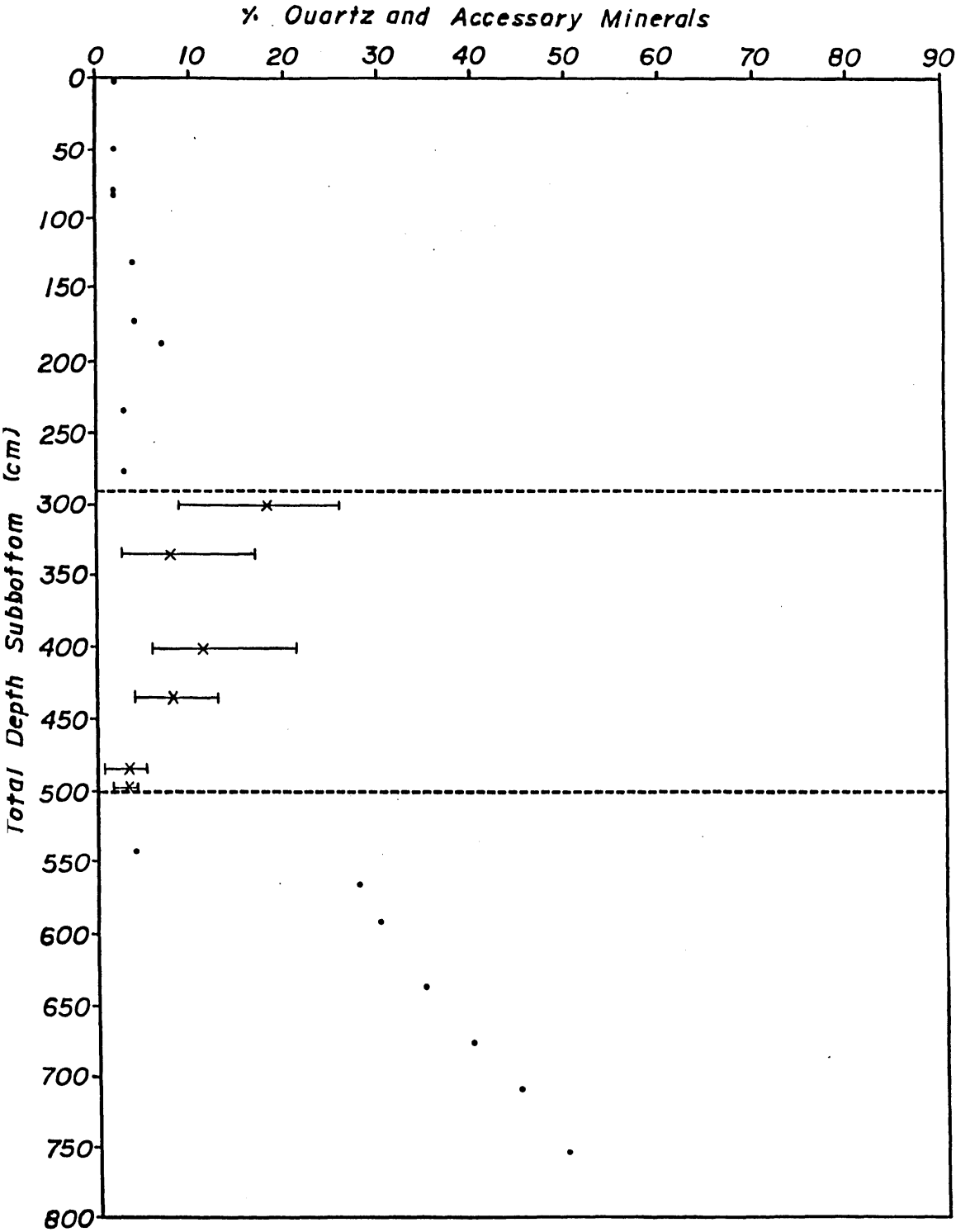

Figure 16: Quartz & Accessory Minerals Abundance (%) Downcore, Lake Caserococha

X-ray Diffraction Analysis: Comparison of Chlorite and Illite.

The diffraction patterns produced during X-ray diffraction analysis of the Lake Caserococha core indicate that the prominent clay minerals in the core are chlorite and illite. On each diffractogram, 7 Å peak of chlorite and 10 Å peak of illite was identified; the areas under these peaks were measured with a polar planimeter, and peak area ratios were calculated to provide a measure of the relative importance of chlorite and illite in each sample. Chlorite/illite peak area ratios are recorded in Appendix III, and the ratios have been plotted as a downcore profile of relative chlorite and illite abundances (Figure 17). Sharp fluctuations in the chlorite to illite ratios occur downcore, with the most significant change occurring between 172.5 cm and 276.0 cm, where the ratio climbs from .2667 to 1.2000, respectively. The ratio then decreases to .5000 at 342.5 cm. In a general sense, the relative abundance of chlorite increases downcore; this trend can be identified in Figure 17, along with the shorter-term fluctuations described previously.

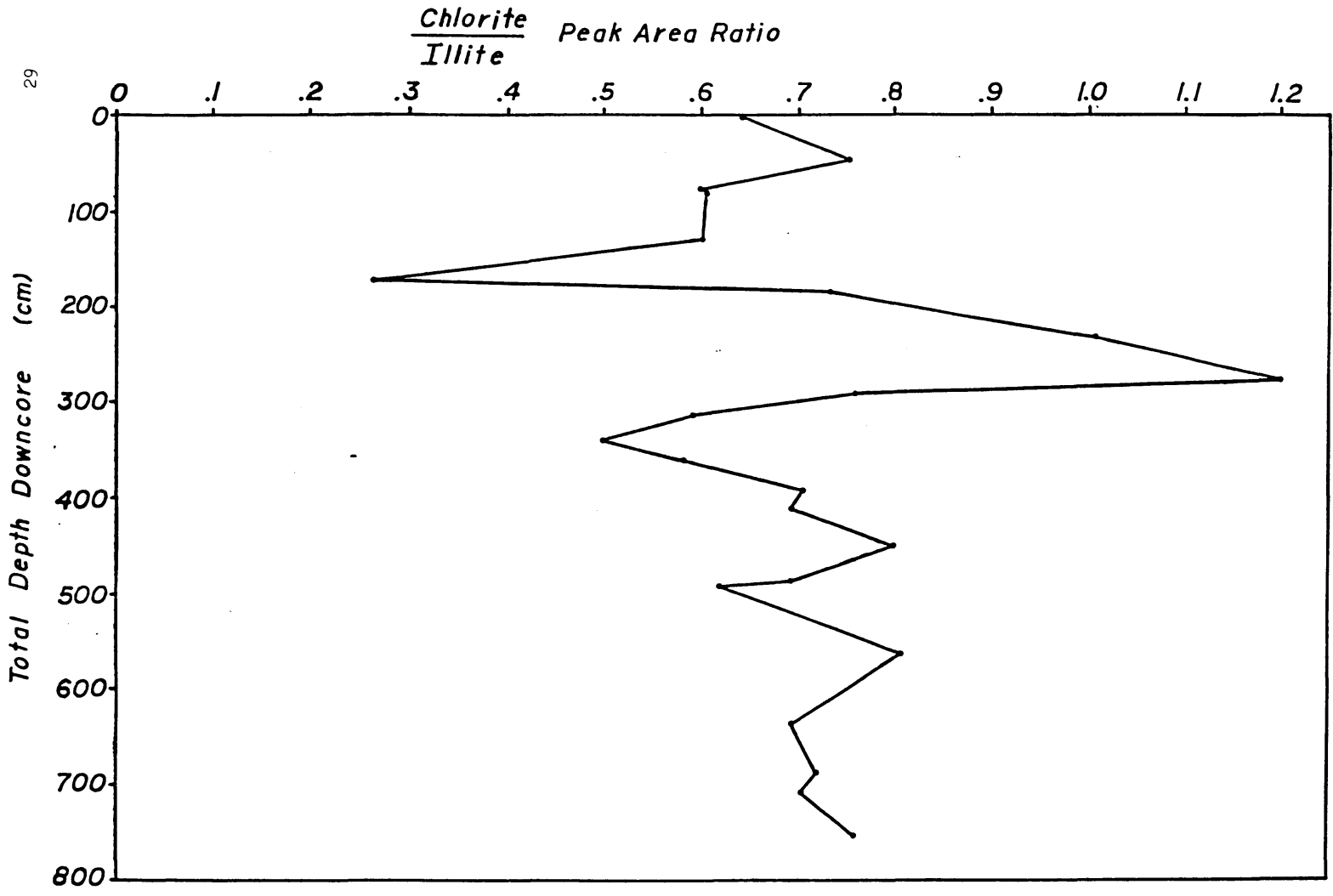

Figure 17: $\frac{\text{Chlorite}}{\text{Illite}}$ Peak Area Ratio

DISCUSSION

Previous Studies Similar to Lake Caserococha Investigation

An investigation attempting to determine the date of deglaciation in Hidden Lake, Alaska, was published by Rymer and Sims (1982). These researchers found a distinct change in sediment characteristics at a particular depth in a core of the lake's sediments. This variation suggested that a change in the depositional environment had occurred, and was recorded by the boundary between the two lithologies. Rymer and Sims interpreted this change to reflect the response of sedimentary processes to the recession of the glacier that deposited material into the then-proglacial Hidden Lake. They concluded that an abrupt environmental change is reflected in a sediment core by changes in lithology, including changes in the abundance of biogenics and clays, especially chlorite (Rymer and Sims, 1982).

In an earlier study similar to that of Rymer and Sims, Karlen (1981) concluded that the sediments of lakes having glaciers in their drainage basins differ greatly from sediments in other lakes, in that the inorganic content fluctuates considerably in ice-controlled lakes. These fluctuations, in turn, are caused by fluctuations in glacier activity (Karlen, 1981).

Ashley (1975) described varves in glacial Lake Hitchcock. She presented data suggesting that the seasonally-deposited varves of Lake Hitchcock consist of a summer silty layer and a winter clay layer. (Ashley, 1975).

The results of these three studies suggest that glacially-influenced lakes are characterized by seasonal fluctuations in the importance of biogenic and inorganic sedimentary components, and by the presence of abundant chlorite. Lakes free of glacial influence, however, contain less-variable

sediments, and contain less chlorite. The Lake Caserococha sediments will now be examined for these indicators, in order to interpret the paleoclimatic record preserved in Lake Caserococha.

Core Logs

The core logs indicate the presence of three major sediment types within the core, and suggest that the core can be divided into three sections, upper, middle, and lower thirds, based upon the presence of these lithologies. These lithologies agree in gross characteristics with the lithologies identified previously by Colinvaux (Figure 1). The upper third can generally be described as a homogeneous, dark brown/black clay, with an absence of laminae. The top 296 cm appear to be organic-rich, based upon the dark color and the presence of plant fragments near the top of the core.

In this upper third of the core, the homogeneous appearance may reflect a lack of seasonal variation in sediment input during its time of deposition within a climatically "stable" lake. Alternatively, the homogeneous appearance may indicate the effect of bioturbation on these sediments, destroying all rhythmic banding subsequent to deposition. Compositional data discussed below, however, suggest that the homogeneous appearance is a primary depositional feature.

The middle section (296 to 498 cm) contains many thin, alternating light and dark laminae that are moderately- to well-defined. These laminae may represent seasonal fluctuations in sediment input controlled by a nearby glacier; if so, these bands can be termed "varves." However, this generally banded appearance may also reflect fluctuations in sediment input that are not entirely seasonally-controlled. There is a possibility, for example,

that these laminae result from storm deposition. Because storms occur sporadically, and may sometimes occur several times during one year, laminated sediments deposited because of storm activity should not be labeled "varves"; instead, this term should strictly indicate seasonally-varying deposition (Ashley, 1975).

Because the horizon at 452 cm is dated at approximately 12,000 ^{14}C y.b.p., this lithology appears to have been deposited while a glacier was retreating at the Pleistocene-Holocene boundary. This glacial recession would provide major runoff of meltwater, which could be favorable for varve development. Compositional data from adjacent bands will be discussed below; these data suggest that most of the banding does record seasonally-varying deposition (i.e., the formation of varves).

Average Composition Throughout the Core

Table 1 clearly illustrates the downcore decrease in biogenic content, from the organic-rich clay to the organic-poor, unsorted glacial debris. These data also indicate a high percentage of quartz near the bottom of the core in the till, with fluctuating quartz abundance elsewhere. Sedimentary quartz can develop as a product of either physical or chemical weathering, while non-chlorite clays generally develop during chemical weathering. As a result of the dominance of physical weathering in the lower till section, there should be an abundance of quartz present at the bottom, as shown in Table 1. In addition, chlorite is also generally developed during physical weathering; the increase in chlorite/illite ratios with depth (Figure 17) also suggests an increase in the importance of physical weathering in the past.

Table 1 also provides a good indication of the locations of abundant ash in the core. These ash-rich zones occur at 498.0 cm to 499.5 cm and at 472.0 cm to 479.5 cm, corresponding to the white bands described in the core log, sections five and six.

Relative clay abundance varies randomly from 37% to 57% in the eight sets of samples. This pattern allows no conclusions to be drawn from the clay abundance downcore.

Triangle Plots: Comparative Abundance of Three Constituents

In general, each triangle plot (figures 10 through 12) indicates a high biogenic abundance in sets 1 through 3, progressively lower biogenic content in sets 4 through 8, and essentially no biogenics in set 8. This decrease in abundance of biogenous material downcore supports the hypothesis that sediment deposition becomes gradually less controlled by glaciation from the bottom to the top of the core. The increase in biogenics indicates the development of progressively warmer and more productive environments, less ice-controlled than the environment represented by the till section of the core, where little or no biogenic material occurs. This conclusion agrees with the conclusion of Rymer and Sims (1982) that sediments rich in organic matter begin to be deposited after a glacier recedes from the lake's drainage basin and glacial debris is no longer introduced into the lake. Karlen (1981) concludes that the high organic content in a lake following glacial recession records two inputs: much organic material is washed into the lake from the surrounding area, and high organic production occurs within the lake because little glacial debris is suspended in the water to block the light necessary for photosynthesis. Biogenics resulting from both types of input are found in

the upper organic-rich section of the Lake Caserococha sediment core: plant fragments, which are washed into the lake, and diatoms, which are phytoplankton produced within the lake.

Another important generalization can be made by observing ash abundance downcore. Sets 1 through 5 contain relatively little ash compared to sets 6 through 8, where ash bands were seen in the X-radiograph. The sediment directly above the most recent ash bands was radiocarbon-dated at 15,330 $\pm$ 210 y.b.p. This date suggests that the last major period of volcanic activity that affected the lake's sediment deposition occurred just prior to 15,330 y.b.p. Lack of discrete ash bands in the upper cores could be caused by bioturbation of the upper homogeneous sediments.

Clay and quartz abundances show parallel patterns downcore, as indicated in the triangle plots. The magnitude of each constituent varies throughout the core, with a notable increase in both clay and quartz abundances in the eighth set (540.5 cm to 753.0 cm), corresponding to the till.

In summary, the triangle plots appear to be useful in distinguishing the three major lithologic sections of the core. It should be noted that, in comparing the three major constituents in a triangle plot, at least one of the constituents should have a different pattern of occurrence than the others. For example, it is not useful to compare quartz, clay, and ash in this investigation, because each occurs in generally the same pattern: random throughout most of the core, with a higher content in the bottom one or two sets. Thus, the resultant graph shows individual sets clustered and overlapping one another, with no distinction between the three major lithologies.

Downcore Abundances of Four Major Constituents

Overall, the four plots of component abundance vs. depth downcore supplement the conclusions drawn from the table of average compositions (Table 1) and the triangle plots (Figures 10 through 12). Figure 13 shows that the percentage of ash remains low throughout most of the core, but increases from 480 cm to 500 cm, corresponding to a period of active tectonism, as mentioned in the previous discussion.

Conclusions drawn from Figures 14 through 16 are similar to those conclusions previously mentioned about clay, biogenics, and quartz: in general, clay abundance increases downcore, but the increase is not dramatic at any one place on the core, perhaps due partly to dilution by biogenics at the top of the core; biogenics decrease in abundance overall downcore at a steady rate, until the core is devoid of biogenics in the bottom three meters, where till was deposited by the ice prior to formation of the lake; quartz and accessory minerals increase downcore, with the most steady increase in the bottom three meters, corresponding to the till.

Compositional Variations Within the Banded Sections of the Core

Figures 18 through 23 compare the abundances of clay and biogenics in adjacent laminae within six banded sections of the Lake Caserococha core: 296.5 cm to 303.9 cm, 328.0 cm to 336.8 cm, 398.8 cm to 402.5 cm, 430.8 cm to 435.4 cm, 472.0 cm 479.5 cm, and 498.0 cm to 499.5 cm. In each figure, a general pattern can be identified that shows an inverse variation between clay and biogenic abundances within each lamina. This compositional variation suggests that the laminae are actually varves, with seasonally-fluctuating influxes of clay and biogenics. During the summer, when meltwater flow

occurs, but phytoplankton productivity is high, lake sediments are deposited with a high abundance of biogenics. During the winter, the lake is ice-covered and calm, but photosynthetic activity is extremely low. As a result, the only sediments deposited are clays, settling out of suspension following input during spring run-off.

X-ray Diffraction Analysis: Comparison of Chlorite and Illite

The presence of chlorite, which is widely accepted to be a direct indication of glaciation, was compared with illite, in order to locate horizons in the core with high chlorite abundances (Figure 17). Drastic increases and decreases in the chlorite to illite ratio can be noted in short distances downcore, indicating that rapid changes occurred during periods of deposition.

The most significant change occurs between 172.5 cm and 276 cm downcore, where the chlorite to illite peak are ratio decreases from 1.2000 at 276.0 cm to .2667 at 172.5 cm. This change corresponds to the termination of the banded section. These changes, the rapid upward decrease in chlorite content and the change in style of deposition, both suggest that retreat of the glacier beyond the zone of direct influence upon lake sedimentation occurred at this time. The laminated section marks a period of time when the glacier was close enough to the lake to control sediment input and productivity, but did not physically encroach upon the lake. The upper homogeneous section, on the other hand, was deposited under more distal proglacial conditions, without any major or direct glacial influence. Environmental conditions of less ice resulted in higher productivity and more oxygen in the water column, resulting in deposition of organic-rich sediments. Bioturbation, or mixing of the sediment by burrowing organisms, explains the occurrence of homogeneous sediments.

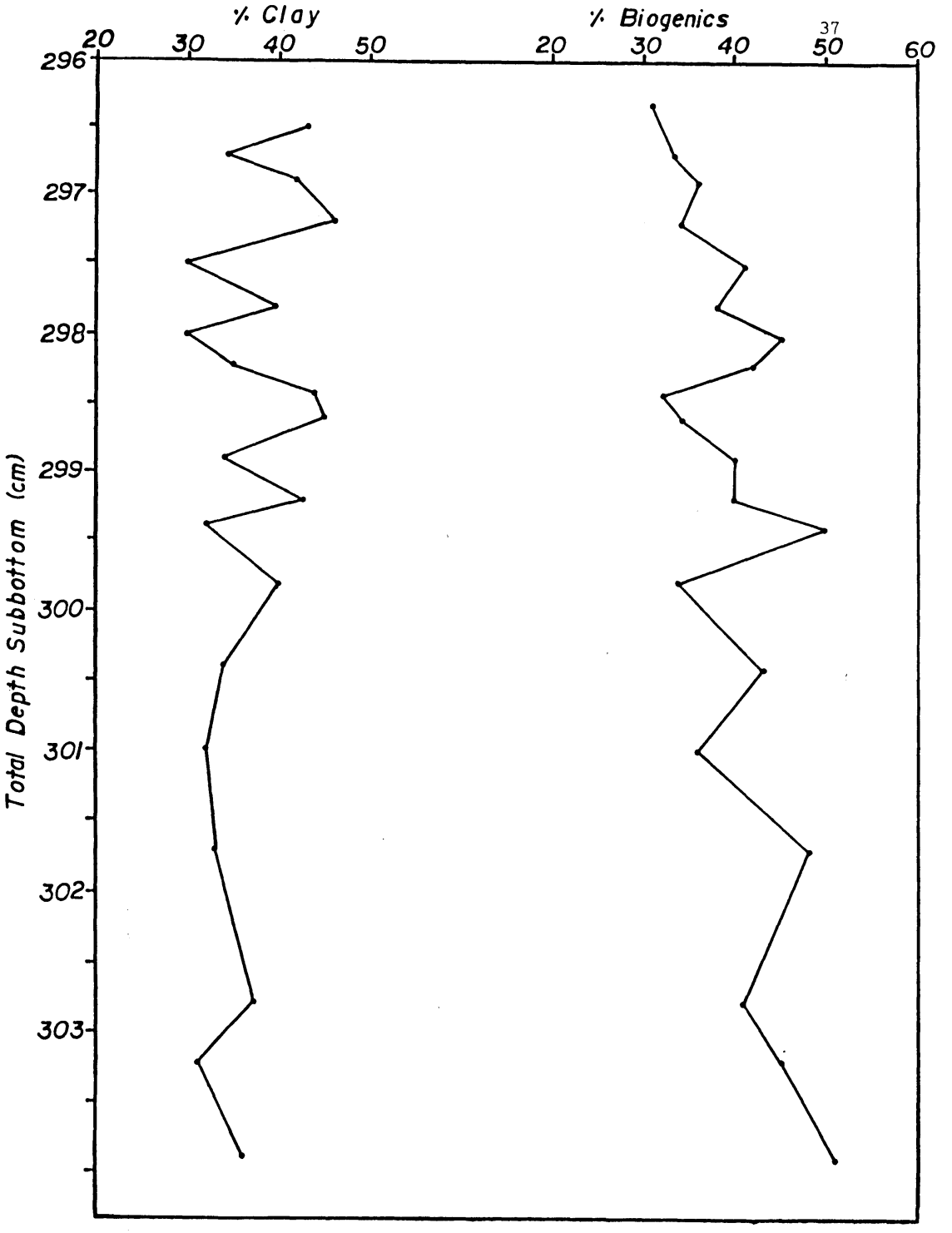

Figure 18: Detailed Plot of Clay and Biogenic Abundances in Adjacent Laminae of Set 2

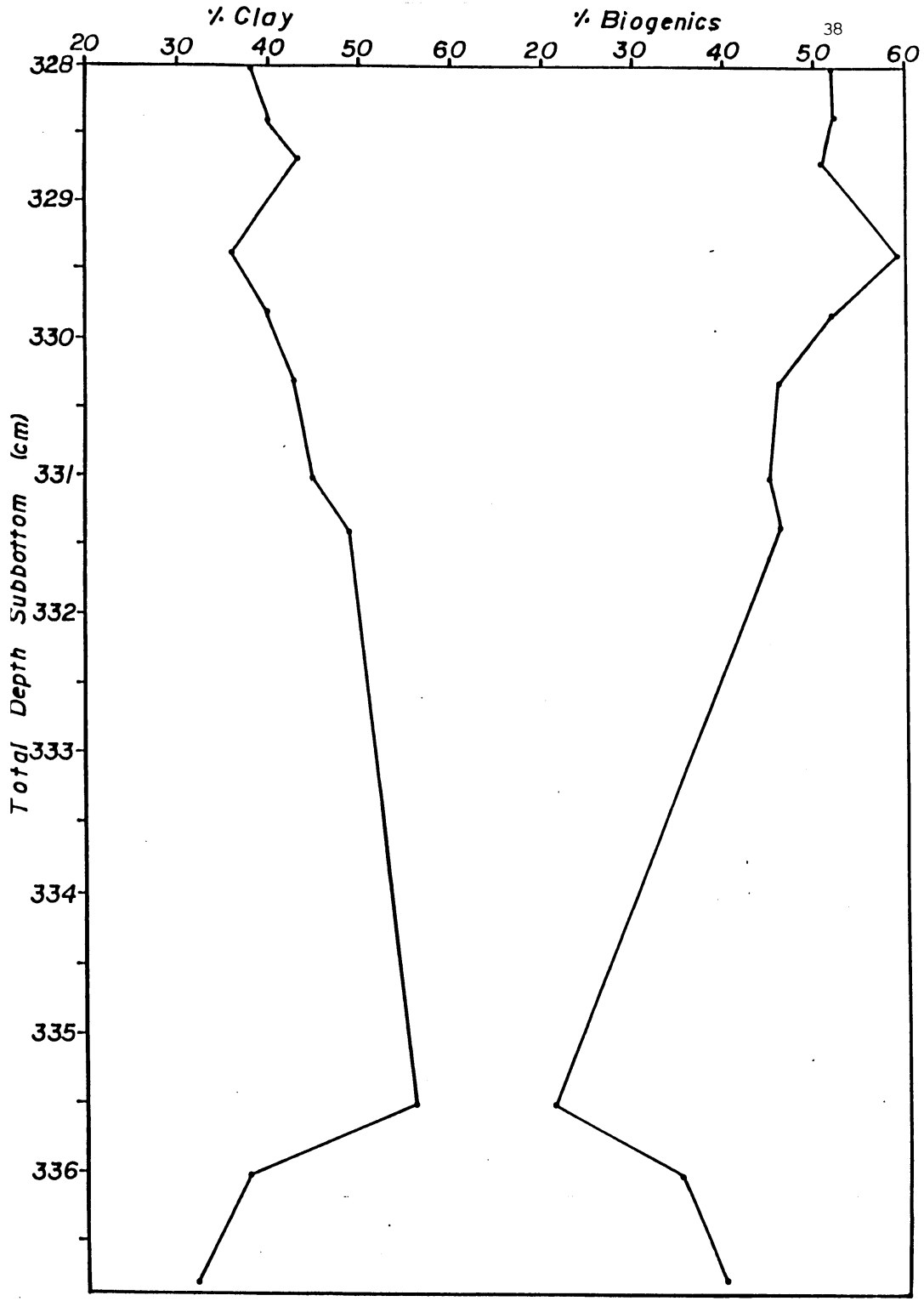

Figure 19: Detailed Plot of Clay and Biogenic Abundances in Adjacent Laminae of Set 3

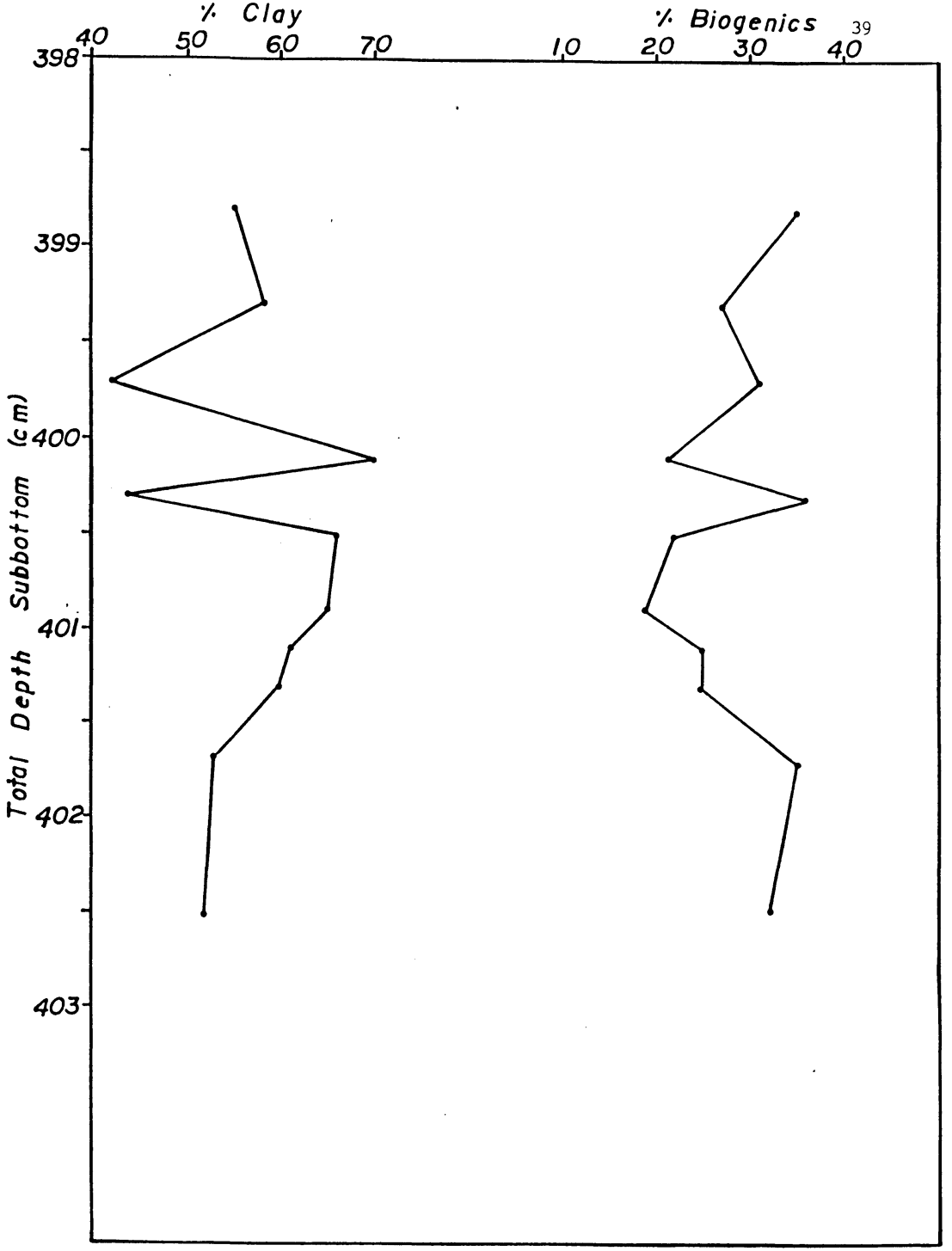

Figure 20: Detailed Plot of Clay and Biogenic Abundances in Adjacent Laminae of Set 4

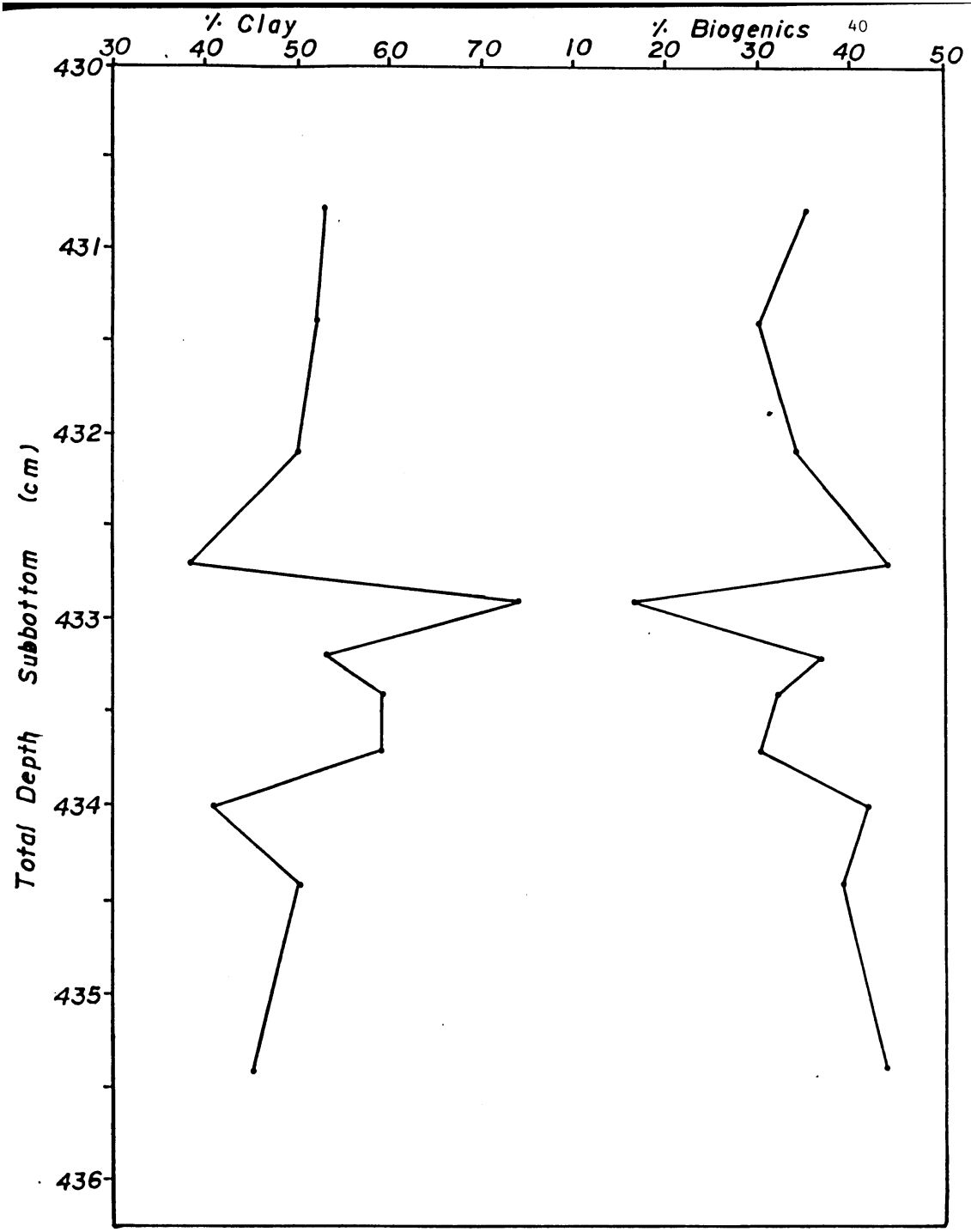

Figure 21: Detailed Plot of Clay and Biogenic Abundances in Adjacent Laminae of Set 5

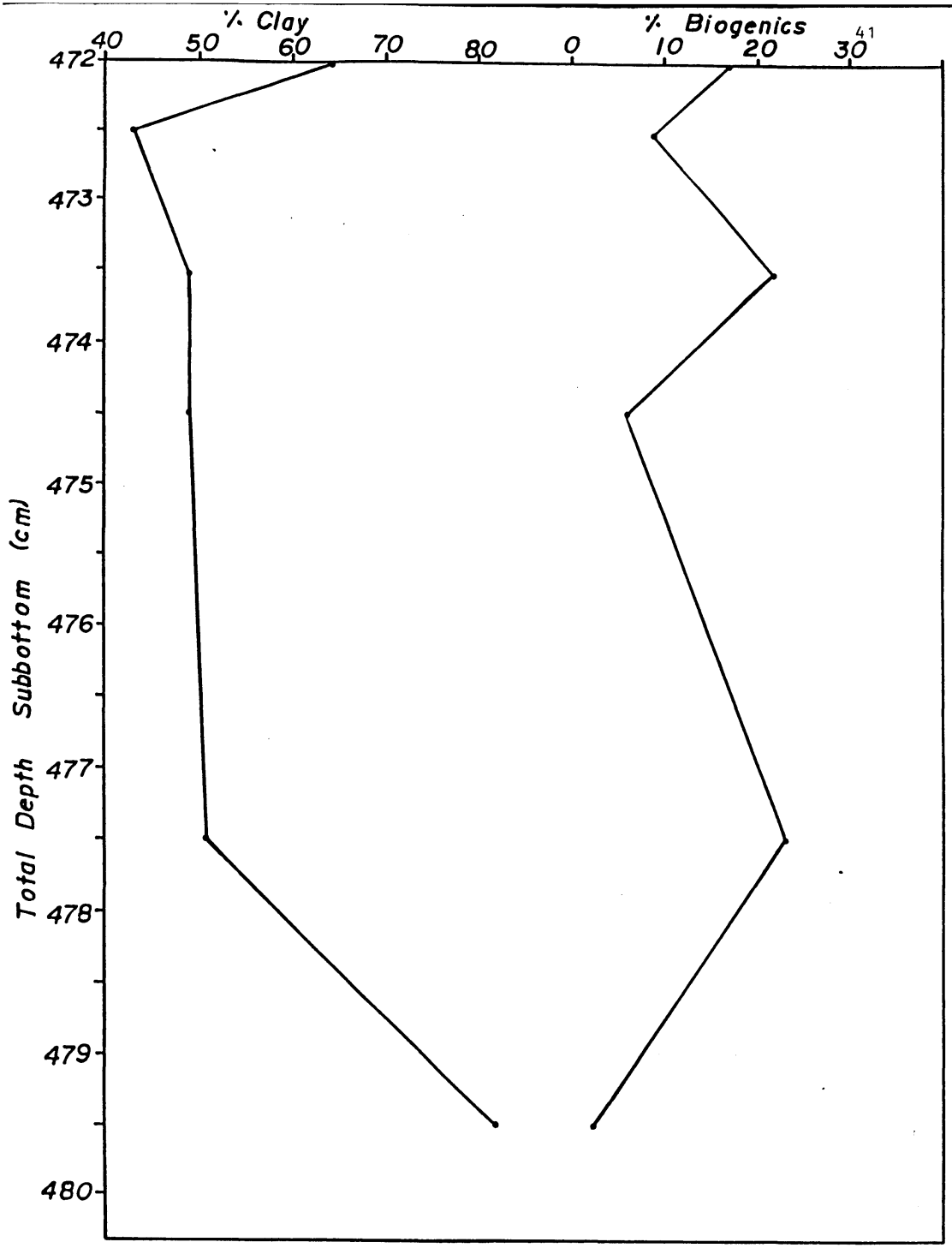

Figure 22: Detailed Plot of Clay and Biogenic Abundances in Adjacent Laminae of Set 6

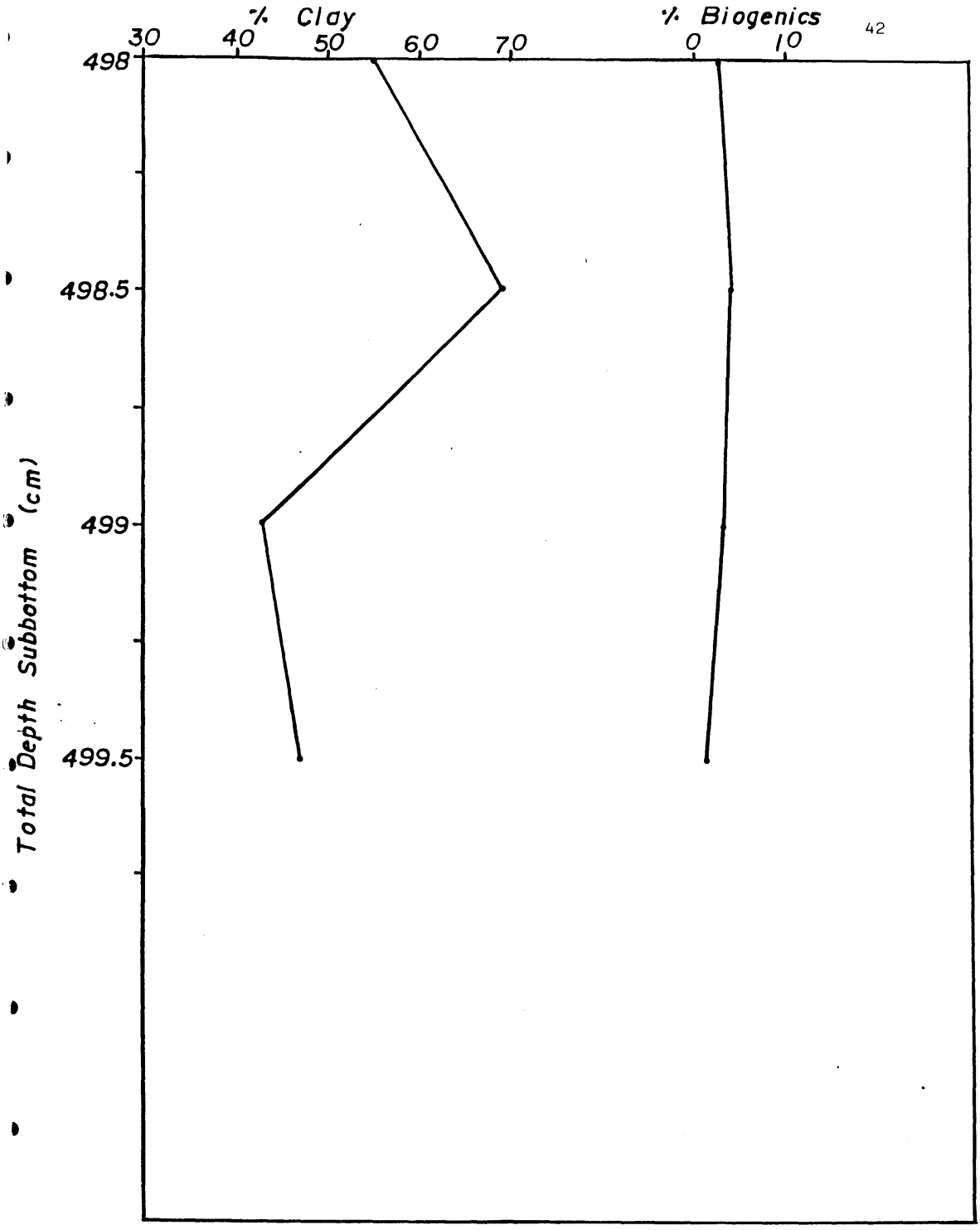

Figure 23: Detailed Plot of Clay and Biogenic Abundances in Adjacent Laminae of Set 7

CONCLUSIONS

1. The glaciolacustrine sediments of Lake Caserococha, Peru, can be divided into three distinct, lithologic sections downcore: an upper homogeneous, organic-rich section; a middle banded section of clays and silts; and a lower inorganic section of till, including particles of clay, silt, sand, and gravel size.

2. Chlorite to illite peak area ratio values are high in the ice-controlled sediments and decrease rapidly up-section toward the non-glacial sediments.

3. The deglaciation of the Lake Caserococha basin occurred at approximately 12,000 ^{14}C y.b.p., corresponding to the transition from the upper part of the homogeneous section.

4. The laminae in the Lake Caserococha sediments, located between 290 cm and 500 cm downcore, probably represent seasonal varves, each with inverse proportions of clay to biogenic abundance; however, some of these laminae may also represent storm deposits.

BIBLIOGRAPHY

Ashley, G. M. "Rhythmic Sedimentation in Glacial Lake hitchcock, Massachusetts-Connecticut." Glaciofluvial and Glaciolacustrine Sedimentation, S.E.P.M. Special Publ. vol. 23 (1975), 305-320.

Colinvaux, P. S. "climate and the Galapagos Islands." Nature, vol. 240 (1972), 17-20.

Heusser, C. J. "Vegetation and Climate of the Southern Chilean Lake District." Quaternary Research, vol. 4 (1974), 290-315.

Ludlam, S. D. "Rhythmic Deposition in Lakes of the Northeastern United States." Moraines and Varves, (1979), 195-302.

Karlen. "Lacustrine Sediment Studies." Geographiska Annaler, vol. 63A (1981), 273-281.

Rymer, M. K., and J. D. Simms. "Lake-sediment Evidence for the Deglation of Hidden Lake area, Kenai Peninsula, Alaska." Geology, vol. 10 (1982), 314-316.

van der Hammen, T. "The Pleistocene Change of Vegetation and Climate in Tropical South America." Journal of Biogeography, vol. 1 (1974), 3-26.

Appendix I: Sample Locations in the Lake Caserococha Core

#	Section-Depth in Section (cm)	Total Depth Subbottom (cm)	#	Section-Depth in Section (cm)	Total Depth Subbottom (cm)
1.	1-1	1	31.	4-44.9	328.4
2.	1-50	50	32.	4-45.2	328.7
3.	1-90	79	33.	4-45.9	329.4
4.	2-2	83.5	34.	4-46.3	329.8
5.	2-50	131.5	35.	4-46.8	330.3
6.	2-91	172.5	36.	4-47.5	331.0
7.	3-2	185.0	37.	4-47.9	331.4
8.	3-50	233.0	38.	4-52.0	335.5
9.	3-93	276.0	39.	4-52.5	336.0
10.	4-13	296.5	40.	4-53.3	336.8
11.	4-13.2	296.7	41.	5-14.3	398.8
12.	4-13.4	296.9	42.	5-14.8	399.3
13.	4-13.7	297.2	43.	5-15.2	399.7
14.	4-14.0	297.5	44.	5-15.6	400.1
15.	4-14.3	297.8	45.	5-15.8	400.3
16.	4-14.5	298.0	46.	5-16.0	400.5
17.	4-14.7	298.2	47.	5-16.4	400.9
18.	4-14.9	298.4	48.	5-15.6	401.1
19.	4-15.1	298.6	49.	5-16.8	401.3
20.	4-15.4	298.9	50.	5-17.2	401.7
21.	4-15.7	299.2	51.	5-18.0	402.5
22.	4-15.9	299.4	52.	5-46.3	430.8
23.	4-16.3	299.8	53.	5-46.9	431.4
24.	4-16.9	300.4	54.	5-47.6	432.1
25.	4-17.5	301.0	55.	5-48.2	432.7
26.	4-18.2	301.7	56.	5-48.4	432.9
27.	4-19.3	302.8	57.	5-48.7	433.2
28.	4-19.7	303.2	58.	5-48.9	433.4
29.	4-20.4	303.9	59.	5-49.2	433.7
30.	4-44.9	328.0	60.	5-49.5	434.0

Appendix I (continued)

#	Section-Depth in Section (cm)	Total Depth Subbottom (cm)
61.	5-49.9	434.4
62.	5-50.9	435.4
63.	5-87.5	472.0
64.	5-88.0	472.5
65.	5-89.0	473.5
66.	5-90.0	474.5
67.	5-93.0	477.5
68.	5-95.0	479.5
69.	6-18.5	498.0
70.	6-19.0	498.5
71.	6-19.5	499.0
72.	6-20.0	499.5
73.	6-61.0	540.5
74.	6-88.0	567.5
75.	7-5.0	590.0
76.	7-50.0	635.0
77.	7-92.5	677.5
78.	8-21.0	709.0
79.	8-65.0	753.0

Appendix II: Composition of Lake Caserococha Sediments
(% by Smear Slide Analysis)

#	Section-Depth in Section (cm)	Plant Material	Diatoms	Clay	Ash	Quartz & Accessory Minerals	Opaque Minerals
1.	1-1.0	64	12	20	2	1	1
2.	1-50.0	15	20	62	1	1	1
3.	1-90.0	18	15	64	1	1	1
4.	2-2.0	39	35	22	2	1	1
5.	2-50.0	30	39	26	1	3	1
6.	2-91.0	6	48	41	1	3	1
7.	3-2.0	10	19	63	1	5	2
8.	3-50.0	15	24	57	1	1	2
9.	3-93.0	20	20	45	12	1	2
10.	4-13.0	6	25	43	5	20	1
11.	4-13.2	3	30	34	8	25	0
12.	4-13.4	6	30	42	6	15	1
13.	4-13.7	4	30	46	4	15	1
14.	4-14.0	8	33	30	8	20	1
15.	4-14.3	3	35	40	5	15	2
16.	4-14.5	5	43	30	6	15	1
17.	4-14.7	4	38	35	2	20	1
18.	4-14.9	2	30	44	3	20	1
19.	4-15.1	1	33	45	5	15	1
20.	4-15.4	0	40	34	5	20	1
21.	4-15.7	0	40	43	4	12	1
22.	4-15.9	5	45	32	5	12	1
23.	4-16.3	1	33	40	2	23	1
24.	4-16.9	1	42	34	2	20	1
25.	4-17.5	4	32	32	6	25	1
26.	4-18.2	5	43	33	3	15	1
27.	4-19.3	1	40	37	6	15	1
28.	4-19.7	2	43	32	4	18	1
29.	4-20.4	1	50	36	4	8	1
30.	4-44.5	2	50	38	3	6	1

Appendix II (continued)

#	Section-Depth in Section (cm)	Plant Material	Diatoms	Clay	Ash	Quartz & Accessory Minerals	Minerals
31.	4-44.9	5	47	40	2	6	0
32.	4-45.2	1	50	43	2	4	0
33.	4-45.9	4	55	36	1	3	1
34.	4-46.3	1	51	40	2	5	1
35.	4-46.8	6	40	43	2	8	1
36.	4-47.5	3	42	45	2	7	1
37.	4-47.9	2	44	49	2	3	0
38.	4-52.0	1	20	56	12	10	1
39.	1-52.5	6	29	38	10	15	2
40.	4-53.3	5	35	32	5	10	3
41.	5-14.3	10	25	55	3	5	2
42.	5-14.8	5	22	58	6	8	1
43.	5-15.2	9	22	42	5	20	2
44.	5-15.6	3	18	70	3	5	1
45.	5-15.8	6	30	44	4	15	1
46.	5-16.0	2	20	66	6	5	1
47.	5-16.4	4	15	65	5	10	1
48.	5-16.6	10	15	61	4	8	2
49.	5-16.8	8	17	60	6	8	1
50.	5-17.2	20	15	53	4	7	1
51.	5-18.0	20	12	52	4	10	2
52.	5-46.3	2	33	53	4	6	2
53.	5-46.9	5	25	52	6	10	2
54.	5-47.6	4	30	50	6	9	1
55.	5-48.2	8	36	38	4	11	3
56.	5-48.4	4	12	74	3	5	2
57.	5-48.7	9	28	53	5	4	1
58.	5-48.9	7	25	59	5	3	1
59.	5-49.2	5	25	59	5	4	2
60.	5-49.5	9	33	41	6	10	1

Appendix II (continued)

#	Section-Depth in Section (cm)	Plant Material	Diatoms	Clay	Ash	Quartz & Accessory Minerals	Minerals
61.	5-49.9	5	34	50	4	6	1
62.	5-50.9	11	33	45	5	5	1
63.	5-87.5	15	2	64	15	3	1
64.	5-88.0	7	2	43	45	2	1
65.	5-89.0	20	2	49	25	4	0
66.	5-90.0	5	1	49	40	4	1
67.	5-93.0	22	1	51	22	4	0
68.	5-95.0	2	0	82	15	1	0
69.	6-18.5	2	1	55	38	3	1
70.	6-19.0	4	0	69	23	2	2
71.	6-19.5	3	0	43	50	2	2
72.	6-20.0	1	0	47	50	1	1
73.	6-61.0	1	0	47	48	2	2
74.	6-88.0	0	0	64	8	20	8
75.	7-5.0	0	0	60	10	10	20
76.	7-50.0	0	0	50	15	20	15
77.	7-92.5	0	0	50	10	20	20
78.	8-21	0	0	35	20	30	15
79.	8-65	0	0	35	15	35	15

Appendix III: Chlorite and Illite Data by X-ray Diffraction Analysis

Section-Depth in Section (cm)	Total Depth Subbottom (cm)	Area Under Chlorite Peak	Area Under Illite Peak	$\frac{\text{Chlorite}}{\text{Illite}}$
1-1	1	54	84	.6429
1-49	49	15	20	.7500
1-89	79	12	20	.6000
2-1	83.5	14	23	.6087
2-49	131.5	9	15	.6000
2-90	172.5	4	15	.2667
3-0	185.0	11	15	.7333
3-49	233 0	12	11	1.0909
3-93	276.0	6	5	1.2000
4-9	292.5	63	83	.7590
4-34	314.5	35	59	.5932
4-59	342.5	14	28	.5000
4-77	360.5	14	24	.5833
5-7	390.5	19	27	.7037
5-29	413.5	27	39	.6923
5-66	450.5	24	30	.8000
6-0	484.5	111	160	.6938
6-7	491.5	87	140	.6214
6-85	564.5	105	130	.8077
7-49	635.0	98	141	.6950
7-93	677.5	137	188	.7287
8-21	709.0	103	146	.7055
8-65	753.0	95	125	.7600